



PLINIO MENDES SENNA

Analyzes of the surface integrity of dental implants and the influence of
nitriding and amino-functionalization treatments on osteogenesis

Análises da integridade da superfície de implantes dentais e da
influência dos tratamentos de nitretação e amino-funcionalização na
osteogênese

Piracicaba

2013



Universidade Estadual De Campinas
Faculdade de Odontologia de Piracicaba

PLINIO MENDES SENNA

Analyzes of the surface integrity of dental implants and the influence of
nitriding and amino-functionalization treatments on osteogenesis

Análises da integridade da superfície de implantes dentais e da
influência dos tratamentos de nitretação e amino-funcionalização na
osteogênese

Thesis presented to the Piracicaba Dental School
of the University of Campinas in partial fulfillment
of the requirements for the degree of Doctor, in
the area of Prosthodontics.

Tese apresentada à Faculdade de Odontologia
de Piracicaba, da Universidade Estadual de
Campinas, para obtenção do título de Doutor em
Clínica Odontológica, Área de Prótese Dental.

Orientadora: Profa. Dra. Altair Antoninha Del Bel Cury

ESTE EXEMPLAR CORRESPONDE À VERSÃO FINAL DA TESE
DEFENDIDA PELO ALUNO PLINIO MENDES SENNA, E ORIENTADA
PELA PROFA. DRA. ALTAIR ANTONINHA DEL BEL CURY.

PIRACICABA

2013

Ficha catalográfica
Universidade Estadual de Campinas
Biblioteca da Faculdade de Odontologia de Piracicaba
Josidelma Francisca Costa de Souza - CRB 8/5894

Se58a Senna, Plinio Mendes, 1984-
Analyzes of the surface integrity of dental implants and the influence of
nitriding and amino-functionalization treatments on osteogenesis / Plinio Mendes
Senna. – Piracicaba, SP : [s.n.], 2013.

Orientador: Altair Antoninha Del Bel Cury.
Tese (doutorado) – Universidade Estadual de Campinas, Faculdade de
Odontologia de Piracicaba.

1. Implantes dentários. 2. Osseointegração. I. Del Bel Cury, Altair
Antoninha, 1948-. II. Universidade Estadual de Campinas. Faculdade de
Odontologia de Piracicaba. III. Título.

Informações para Biblioteca Digital

Título em outro idioma: Análises da integridade da superfície de implantes dentais e da
influência dos tratamentos de nitretação e amino-funcionalização na osteogênese

Palavras-chave em inglês:

Dental implants

Osseointegration

Área de concentração: Prótese Dental

Titulação: Doutor em Clínica Odontológica

Banca examinadora:

Altair Antoninha Del Bel Cury [Orientador]

Hélio Rodrigues Sampaio Filho

Emmanuel João Nogueira Leal da Silva

Bruno Salles Sotto Maior

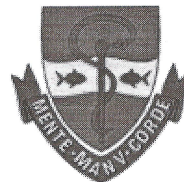
Luiz Augusto Duarte Meirelles

Data de defesa: 19-12-2013

Programa de Pós-Graduação: Clínica Odontológica



UNIVERSIDADE ESTADUAL DE CAMPINAS
Faculdade de Odontologia de Piracicaba



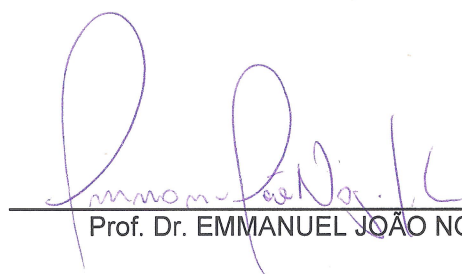
A Comissão Julgadora dos trabalhos de Defesa de Tese de Doutorado, em sessão pública realizada em 19 de Dezembro de 2013, considerou o candidato PLINIO MENDES SENNA aprovado.



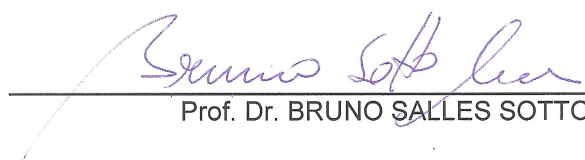
Profa. Dra. ALTAIR ANTONINHA DEL BEL CURY



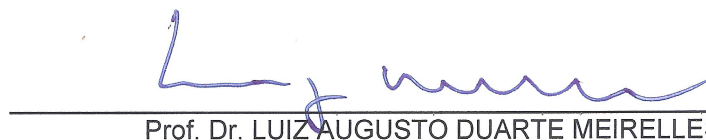
Prof. Dr. HÉLIO RODRIGUES SAMPAIO FILHO



Prof. Dr. EMMANUEL JOÃO NOGUEIRA LEAL DA SILVA



Prof. Dr. BRUNO SALLES SOTTO MAIOR



Prof. Dr. LUIZ AUGUSTO DUARTE MEIRELLES

Abstract

Dental implants receive surface treatments to create micro- and nano-structures on surface to increase the contacting area with bone, which favors osseointegration. However, the resistance of these structures in face of the friction against the bone tissue during the implant insertion is not evaluated yet. Thus, the objective in this study was to quantify by means of roughness parameters the surface wear caused by the insertion procedure in the bone tissue and to investigate the presence of loose titanium particles at bone-implant interface (Chapter 1); to evaluate the influence of plasma nitriding treatment on surface properties of titanium and on its biocompatibility (Chapter 2); and to investigate the protein adsorption *in vitro* and osteogenesis around amino-functionalized implants placed in rabbits (Chapter 3). In Chapter 1, roughness of three implants representing different geometries and surface treatments were evaluated by interferometry before and after insertion into bovine rib blocks. The blocks were also evaluated by microscopy to identify titanium particles at the interface. The amplitude of all roughness parameters were smaller after the insertion procedure for all implant groups and microscopic images revealed presence of loose titanium and aluminum particles at the interface, concentrated at the cortical crest. Therefore, it was concluded that moderately rough surfaces can release loose particles at the interface. In Chapter 2, titanium discs (12.7×2 mm) with moderately rough surface were nitrided by cold plasma. Human osteoblasts (SAOS-2) were cultivated on the discs for 1, 3, 5 and 7 days. Cell proliferation and differentiation were evaluated by MTS, production of alkaline phosphatase and by qPCR. It was observed that plasma nitriding increased the nitrogen content on surface, and also hardness, wettability and nanostructures. No significant difference between titanium and nitrided surface was seen on cell behavior. Therefore, it was concluded that nitriding treatment increase surface hardness and does not jeopardize the biocompatibility of titanium. In Chapter 3, titanium was amino-functionalized by 3-aminopropyltriethoxysilane. Protein profile was identified by mass spectroscopy after discs were immersed in human blood

plasma for 3 h. To evaluate osteogenesis, titanium implants (3.75×6 mm) were placed in 10 New Zealand adult rabbits (1 in the femoral distal metaphysis and 2 in the tibial proximal metaphysis of both legs). The animals were sacrificed after 3 and 6 weeks and implants with adjacent bone were collected, fixed and included in resin blocks. After, 20 μ m thick slides were prepared at the central region of each implant and stained by toluidine blue. Histomorphometric analysis consisted of measuring the bone-to-implant contact (BIC). Treated surface exhibited higher amount of adsorbed proteins; however, lower relative abundance of fibronectin. No significant difference was identified between the groups for BIC values after 3 and 6 weeks. Therefore, amino-functionalization enhance protein adsorption but has no effect on early bone formation.

Keywords: Dental implants; Osseointegration.

Resumo

Os implantes dentais recebem diversos tratamentos para criar micro- e nano-estruturas na superfície, aumentando a área de contato com o osso e favorecendo a osseointegração. O objetivo deste trabalho foi quantificar por meio de parâmetros de rugosidade as alterações de superfície causadas pelo processo de inserção no tecido ósseo e investigar a presença de partículas soltas de titânio na interface osso-implante (Capítulo 1); avaliar a influência do tratamento de nitretação por plasma nas propriedades de superfície do titânio e na sua biocompatibilidade (Capítulo 2); e avaliar a adsorção de proteínas *in vitro* e a osteogênese ao redor de implantes amino-funcionalizados instalados em coelhos (Capítulo 3). No Capítulo 1, a rugosidade de três grupos de implantes representando diferenças geometrias e tratamentos de superfície foi avaliada por interferometria antes e após a inserção dos mesmos em blocos de costela bovina. Os blocos também foram avaliados por microscopia para identificar partículas de titânio presentes na interface. A amplitude de todos os parâmetros de rugosidade das superfícies dos implantes foram menores após a inserção para todos os grupos e as imagens microscópicas revelaram a presença de partículas de titânio e alumínio na interface, concentradas principalmente no nível do osso cortical. Assim, concluiu-se que as superfícies moderadamente rugosas podem gerar partículas soltas de titânio na interface. No Capítulo 2, discos de titânio (12,7 × 2 mm) moderadamente rugosos foram nitretados por plasma a frio. Osteoblastos humanos (SAOS-2) foram cultivados sobre os discos por 1, 3, 5 e 7 dias. A proliferação e diferenciação celular foram avaliadas por MTS, produção de fosfatase alcalina e por qPCR. Foi observado, que a nitretação aumentou a quantidade de nitrogênio na superfície, além da dureza, molhabilidade e nanoestruturas. Não houve diferença no comportamento celular em relação ao grupo não nitretado. Assim, concluiu-se que a nitretação por plasma a frio aumentou a dureza da superfície e não prejudicou a biocompatibilidade do titânio. No Capítulo 3, o titânio foi amino-funcionalizado com 3-aminopropiltrietoxisilano. O perfil protéico adsorvido foi

avaliado por espectrometria de massas após discos serem imersos em plasma sanguíneo humano por 3 h. Para a análise da osteogênese, implantes de titânio (3,75 × 6 mm) receberam o mesmo tratamento e foram instalados em 10 coelhos New Zealand adultos (1 na metáfise distal do fêmur e 2 na metáfise proximal da tíbia de ambas as patas). Os animais foram sacrificados após 3 e 6 semanas e os implantes e osso adjacente foram coletados, fixados e incluídos em blocos de resina. Em seguida, lâminas de 20 µm de espessura foram preparadas na região central de cada implante e coradas com azul de toluidina. A análise histomorfométrica compreendeu a mensuração da área de contato osso-implante. A superfície tratada apresentou maior quantidade total de proteínas adsorvidas; no entanto, com menor abundância relativa de fibronectina. Não houve diferença para a área de contato osso-implante entre os dois grupos de implantes após 3 e 6 semanas. Assim, concluiu-se que a amino-funcionalização aumentou a quantidade de proteínas adsorvidas, mas não foi efetiva para acelerar a osteogênese.

Palavras-chave: implantes dentais; osseointegração.

Sumário

Dedicatória	xiii
Agradecimentos	xv
Introdução	1
Capítulo 1: <i>Surface damage on dental implants with release of loose particles after insertion into bone</i>	4
Capítulo 2: <i>Early cell response to titanium surface nitrided by plasma ion immersion technique</i>	26
Capítulo 3: <i>Evaluation of protein adsorption in vitro and bone formation in vivo on amino-functionalized titanium surface</i>	42
Considerações gerais.....	59
Conclusão	60
Referências	61
Anexo 1: <i>Certificado de aprovação do Comitê de Ética em Pesquisa Animal</i>	63

Dedicatória

Dedico este trabalho a minha família.

Agradecimentos

Agradecimento especial à **Profa. Dra. Altair Antoninha Del Bel Cury**, minha orientadora, a quem reitero a minha mais sincera admiração. Desde o mestrado tive o privilégio de contar com o seu total e irrestrito apoio, o qual faz diferença na nossa vida acadêmica. Muito obrigado pela confiança depositada.

Ao amigo **Prof. Dr. Luiz Augusto Duarte Meirelles**, a quem agradeço toda a atenção e solicitude recebida durante minha estada em Rochester para o estágio de pesquisa no exterior.

Ao amigo **Prof. Dr. Hélio Rodrigues Sampaio Filho**, principal motivador para investir minha formação na pós-graduação da Faculdade de Odontologia de Piracicaba.

À **Universidade Estadual de Campinas – UNICAMP**, na pessoa do Magnífico Reitor, **Prof. Dr. José Tadeu Jorge**.

À **Faculdade de Odontologia de Piracicaba** da Universidade Estadual de Campinas, na pessoa de seu Diretor, **Prof. Dr. Jacks Jorge Junior**; à **Comissão de Pós-Graduação** da Faculdade de Odontologia de Piracicaba – UNICAMP, na pessoa da sua Presidente, **Profa. Dra. Renata Cunha Matheus Rodrigues Garcia**; ao **Coordenador do Programa de Pós-Graduação em Clínica Odontológica** da Faculdade de Odontologia de Piracicaba – UNICAMP, **Prof. Dr. Marcio de Moraes**, pelo meu doutoramento nesta instituição.

Ao **Eastman Institute for Oral Health** da Universidade de Rochester, na pessoa do seu Diretor, **Dr. Eli Eliav**, pela realização do estágio de pesquisa no exterior.

À **Fundação de Amparo a Pesquisa do Estado de São Paulo – FAPESP**, na pessoa do seu Diretor-Presidente, **Prof. Dr. José Arana Varela**, pela bolsa de doutorado no país (Processo 2010/09308-0) e bolsa de estágio de pesquisa no exterior (Processo 2011/23269-0) concedidas.

Aos amigos **Prof. Dr. Bruno Salles Sotto Maior** e **Prof. Dr Emmanuel João Nogueira Leal da Silva**, que participaram da minha rotina e formação na FOP

Aos amigos **Cindy Goes Dodo** e **Yuri Wanderley Cavalcanti**, pelos auxílios nas técnicas de cultivo celular e análises de biologia molecular.

À **Gislaine Regiane Piton**, técnica do laboratório de PPR, por todo o suporte prestado.

Agradecer não é uma tarefa fácil. Para não correr o risco da injustiça, agradeço de antemão a todos, que mesmo indiretamente, contribuíram para a conclusão deste trabalho.

*Ninguém é tão grande que não possa aprender,
nem tão pequeno que não possa ensinar.*

Esopo

Introdução

O uso de implantes osteointegrados com finalidade protética representa grande conquista para a reabilitação estética e funcional de tecidos e órgãos lesionados. Juntamente com a medicina, a odontologia se beneficiou desta possibilidade, culminando com a criação de uma especialidade voltada para o manejo desta modalidade terapêutica. Assim, os implantes dentários estão se tornando a primeira opção para a reposição de dentes por parte do profissional, bem como por parte do paciente, principalmente pela preservação biológica dos dentes adjacentes ao espaço a ser reabilitado, assim como a preservação da estrutura óssea remanescente do rebordo alveolar (1).

O implante dentário constitui-se de um cilindro de titânio inserido cirurgicamente no interior do osso mandibular, maxilar ou zigomático, funcionando como a porção radicular de um dente, e sobre ele se conecta um pilar artificial onde é fixada a porção coronária substitutiva do dente. O sucesso dos implantes dentários é baseado na osteointegração, definida como “a aposição íntima de osso neoformado e reformado em congruência com o metal, incluindo irregularidades de superfície, de forma que, à análise por microscopia óptica, não haja interposição de tecido conjuntivo ou fibroso e seja estabelecida uma conexão estrutural e funcional direta, capaz de suportar cargas fisiológicas normais sem deformação excessiva e sem iniciar um mecanismo de rejeição” (1).

O período de espera para que ocorra a osteointegração é de 4 a 6 meses, dependendo da qualidade óssea, e somente após este período é que o pilar artificial é instalado sobre o implante. Em algumas situações este período de espera pode se tornar um inconveniente para o paciente pela necessidade de uso de próteses parciais ou totais removíveis, o que gera uma busca por novas superfícies com o intuito de melhorar ou acelerar este processo de osteointegração,

principalmente para sítios de baixa qualidade ósseos onde ancoragem do implante nem sempre é a ideal e o uso de carga imediata é contraindicado (2, 3).

Assim, os implantes modernos apresentam superfície rugosa, com estruturas de altura entre 1 e 2 μm , a qual estimula a formação óssea quando comparadas aos implantes usinados apenas (4). No entanto, a baixa resistência à abrasão do titânio (5) pode fazer com que estas micro-estruturas presentes na superfície se danifiquem durante a inserção dos implantes no tecido ósseo. Apesar de este fenômeno ainda não ter sido explorado, pode explicar a origem de partículas soltas de titânio no tecido conjuntivo adjacente aos implantes (6,7).

Além da necessidade de se avaliar a liberação de partículas de titânio pelos implantes, alguns métodos de tratamento de superfície podem ser interessantes para minimizar esta ocorrência ou substituir a necessidade de superfícies rugosas. Neste sentido, a nitretação, a qual é um método comumente utilizado na metalurgia para aumentar a dureza da superfície de metais (8), pode ser um método interessante para aumentar a resistência mecânica das micro-estruturas presentes na superfície do titânio. No entanto, diversos métodos de nitretação são propostos e a biocompatibilidade deste tratamento precisa ser avaliada.

O titânio apresenta uma superfície levemente negativa (9) e a melhora da osteointegração pode recair na mudança de seu potencial elétrico. Assim, uma alternativa para garantir a osseointegração sem a necessidade de alteração da topografia da superfície pode ser a incorporação de grupamentos funcionais no implante. Neste sentido, a amino-funcionalização pode alterar o potencial elétrico da superfície, estimulando a adsorção de proteínas na superfície (10). No entanto, ainda não foi verificado *in vivo* se estimularia a osseointegração (11, 12).

Considerando a importância dos implantes osteointegrados e a multifatorialidade envolvendo a osteointegração, considerou-se importante o desenvolvimento desse trabalho como forma de adicionar conhecimento a esse tema promissor de pesquisa. Assim, o objetivo deste trabalho foi quantificar por meio de parâmetros de rugosidade as alterações de superfície causadas pelo

processo de inserção no tecido ósseo e investigar a presença de partículas soltas de titânio na interface osso-implante (Capítulo 1); avaliar a influência da nitretação por plasma a frio na dureza e na bioatividade celular (Capítulo 2); e avaliar a osteogênese ao redor de implantes amino-funcionalizados instalados em coelhos (Capítulo 3).

Capítulo 1:

Surface damage on dental implants with release of loose particles after insertion into bone

Plinio Senna, DDS, MS;^a Altair Antoninha Del Bel Cury, DDS, PhD;^b Stephen Kates, MD;^c Luiz Meirelles, DDS, PhD^{d,*}

^a PhD student, Department of Prosthodontics and Periodontology, Piracicaba Dental School, State University of Campinas, Brazil;

^b Professor, Department of Prosthodontics and Periodontology, Piracicaba Dental School, State University of Campinas, Brazil;

^c Professor, Department of Orthopaedics, University of Rochester, Rochester, USA;

^d Professor, Division of Prosthodontics, Eastman Dental Center, University of Rochester, Rochester, USA.

Artigo publicado eletronicamente em 28/11/2013 no periódico Clinical Implant Dentistry and Related Research (doi: 10.1111/cid.12167) (Anexo 1).

ABSTRACT

Background: Modern dental implants present surface features of distinct dimensions that can be damaged during the insertion procedure into bone.

Purpose: The aims of this study were (1) to quantify by means of roughness parameters the surface damage caused by the insertion procedure of dental implants and (2) to investigate the presence of loose particles at the interface.

Materials and Methods: Three groups of dental implants representing different surface topographies were inserted in fresh cow rib bone blocks. The surface roughness was characterized by interferometry on the same area before and after the insertion. SEM-BSD analysis was used to identify loose particles at the interface.

Results: The amplitude and hybrid roughness parameters of all three groups were lower after insertion. The surface presenting predominance of peaks ($S_{sk} > 0$) associated to higher structures (height parameters) presented higher damage associated to more pronounced reduction of material volume. SEM-BSD images revealed loose titanium and aluminum particles at the interface mainly at the crestal cortical bone level.

Conclusions: Shearing forces during the insertion procedure alters the surface of dental implants. Loose metal particles can be generated at bone-implant interface especially around surfaces composed mainly by peaks and with increased height parameters.

Key words: Bone; Dental implants; Surface Properties; Surface Topography; Titanium

INTRODUCTION

The modern dental implants modified by different chemical and/or physical techniques present surfaces with enhanced roughness to improve initial bone formation and bone support over time compared to smooth-turned implants.¹ However, the surface of rougher implants presents higher peaks that can be more likely to break and detach during the insertion procedure into bone. The characterization of surface topography of dental implants based on roughness parameters was introduced by Wennerberg et al. in 1992.² and the analysis of the roughness before and after insertion is a reliable alternative to quantify the extent of wear.³ Previous results indicated a change in surface topography of implants unscrewed after 12 weeks of healing in rabbits.⁴

In vivo experiments indicated loose titanium particles in bone tissue around smooth-turned,^{5, 6} grit-blasted/acid-etched⁶ and plasma-sprayed implants.⁶⁻⁹ More recently, soft tissue biopsies performed in patients after 6 months of implant installation detected Ti particles in the connective tissue facing the dental implants.^{10, 11}

Loose particles released from orthopedic load bearing devices due to wear have been associated with bone loss.^{12, 13} Micro and nano sized titanium particles debris phagocytized by macrophages stimulate the production of pro-inflammatory and pro-osteoclastogenic cytokines including Interleukins 1, 6 and 8 and TNF- α ,¹⁴⁻¹⁶ triggering a chronic inflammatory and foreign body granulomatous reaction accompanied by osteolysis^{17, 18} that culminate with aseptic prosthetic loosening.^{19, 20}

Dental implants do not present bearing artificial surfaces in contact to produce wear debris and the release of metal particles in bone tissue arises from the insertion procedure itself.⁸ The shear forces arising from the friction of self-tapping implants against the bone tissue produce a dynamic shifting of stresses on different locations along the implant, related to the heterogeneity of bone tissue and the geometry of the implants.²¹ Thus, dynamic localized spots are randomly created

during insertion of the implants, generating areas of stress concentration that may compromised the integrity of the surface features and consequently release titanium particles in the bone tissue.

In this scenario, initial bone healing immediately after implant placement could be affected by the presence of these loose particles. The aim of this study was to evaluate the surface damage to different dental implants caused by the insertion procedure itself and evaluate the generation of loose metal particles at the bone-implant interface.

MATERIALS AND METHODS

Fresh cow rib bones pieces were prepared and used immediately. Blocks measuring approximately $20 \times 15 \times 15$ mm were cut with a diamond band saw (model C-40; Gryphon Corporation, Sylmar, CA, USA). Those blocks without 1.5 ± 0.5 mm thickness of cortical bone were excluded to keep the sample with similar thickness of human maxilla and mandible bones.²² Next, each block was sectioned at the midline and the two halves were bound tightly back together to the original configuration by a clamp to allow the insertion of the implant at the midline interface (Figure 1).

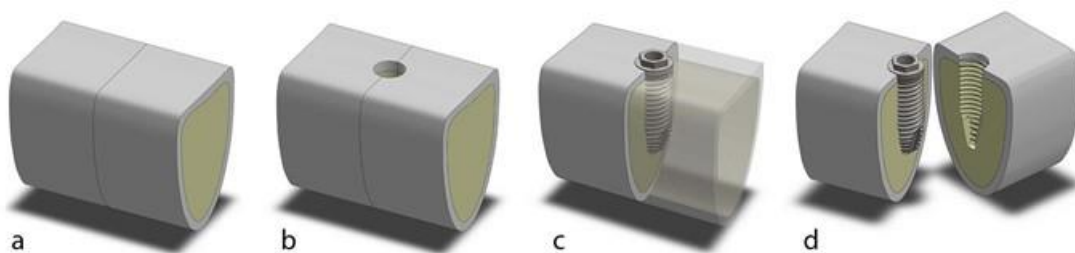


Figure 1. Cow rib bone blocks— $20 \times 15 \times 15$ mm were cut transversely (a) and drilling was performed at the interface, as recommended for dense bone (b). After the implants were fully inserted (c), the blocks were split and the implant was assessed without any additional damage to the implant surface (d).

Cylindrical self-tapping threaded dental implants of similar dimensions and different surface topographies were selected (n = 6 per group): 4.0 × 10 mm TiUnite™ MkIII, Nobel Biocare, Sweden (TU); 4.0 × 11 mm OsseoSpeed™ TX, Astra Tech AB, Sweden (OS) and 4.1 × 10 mm SLActive® Bone Level, Straumann, Switzerland (SL). TU surface features are produced by anodization process, while SL and OS surface features are produced by the combination of grit-blasting and acid-etching processes.²³

The bone blocks were randomly divided and drilling and implant insertion were performed at the interface of the two halves following each manufacturer's instructions with over copious irrigation. The implants were inserted at 25 rpm using the drilling unit (Elcomed SA-310; W&H Dentalwerk Bürmoos GmbH, Bürmoos, Austria). After the implants were fully inserted, the clamp was removed and the blocks were split at the pre-sectioned interface to retrieve the implant, which was easily removed without secondary damage to the surface. The implants were transferred to a plastic tube to be sonicated in purified water (30 min) and acetone (10 min) to remove residual bone debris from the surface.

The crest of all threads, including the microthreads on neck of OS implants, were evaluated at the same regions before and after insertion by interferometry (New View 7300; Zygo, Middlefield, CT, USA) with objective 50× and zoom factor of 0.5. An implant mount (SL implant) and a transfer (TU and OS) was fixed to slide to ensure that the implants were measured at the exact same spot before and after insertion. In addition, careful adjustment was obtained by matching a scratch mark to a pre-determined rectangle mask set on the live display window of the software (MetroPro® version 9.1.2; Zygo) (Figure 2). Band pass Gaussian filter was used to remove errors of form and waviness.

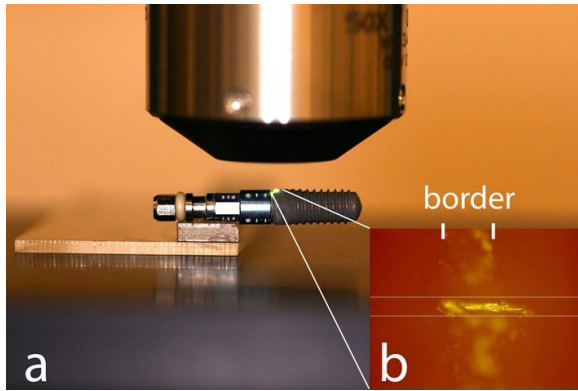


Figure 2. Implant positioning was obtained using the mount fixed to a slide (a). In addition, a scratch mark ensured the exact alignment to a predetermined mask set on the live display window of the software (b).

The roughness parameters selected were calculated using Scanning Probe Image Processor software (version 5.1.8; Image Metrology A/S, Hørsholm, Denmark) and included: amplitude parameters: S_a = average height deviation, and S_{sk} = degree of symmetry of the surface heights about the mean plane (skewness); hybrid parameter: S_{dr} = developed interfacial area ratio; and functional parameters: S_{pk} = peak height above the core roughness; S_k = core roughness height (peak-to-valley) of the surface with the predominant peaks and valleys removed; and S_{vk} = valley depth below the core roughness (Figure 3a).

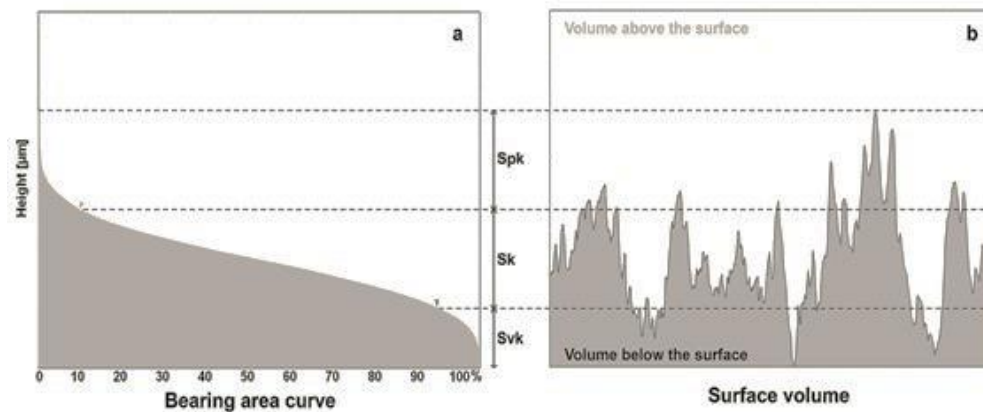


Figure 3. The functional parameters are determined from the bearing area ratio curve (a). S_{pk} corresponds to the peak height above the core roughness; S_k to the core roughness height (peak-to-valley) of the surface with the predominant peaks and valleys removed; and S_{vk} to valley depth below the core roughness. The sum of these parameters ($S_{vk} + S_k + S_{pk}$) determines the total structural height of the surface and the volume of surface features (V_m) comprises 100% of the surface material ratio (b).

In addition, the peak density and the material volume (V_m) correspondent to 100% of the surface features (Figure 3b) were calculated using MetroPro® software. The average difference in V_m ($V_{m_{initial}} - V_{m_{final}}$) calculated by the interferometer was then correlated with the total surface area of the implants to estimate the total volume of particles detached from the surface considering a uniform damage along the entire implant. For this, one implant of each group was subjected to a μ CT scanning (vivaCT 40; Scanco USA Inc., Wayne, PA, USA) to determine the total surface area of the implant, which revealed 173.31, 176.71 and 158.22 mm² for TU, OS and SL groups. From the total volume estimated, the mass of particles was calculated considering the density of titanium dioxide as 4.23 g/cm³.

Scanning electron microscopy (SEM) images of the implants before and after insertion was performed (Zeiss Auriga SEM/FIB, Oberkochen, Germany) at different magnifications, associated to back-scattered electron detector (BSD) and energy-dispersive x-ray spectroscopy (EDS). To detect the presence of loose titanium particles along the bone implantation sites, the bone blocks were dried at 37°C for 48 h after implant removal and evaluated by BSD/EDS. Remaining debris on the bone surface related to the insertion procedure were removed prior to SEM-EDS with a jet spray to avoid unstable structures that would compromise the analysis and contaminate the electron microscope vacuum chamber.

The roughness parameters, peak density and V_m data before and after implant insertion was analyzed by paired t-test ($\alpha = 0.05$) (SPSS Statistics 20; IBM Corporation, Armonk, New York, USA).

RESULTS

Implant insertion torque never exceeded the maximum value recommended by the manufactures. Average insertion torque (Ncm) of 40.4(2.0), 35.2(3.1) and 36.5(2.5) was calculated for TU, OS and SL implants, respectively.

The average height deviation (S_a) of the TU, OS and SL implants demonstrated a reduction of 0.1-, 0.06- and 0.2 μ m after insertion (Figure 4). The degree of symmetry measured by the S_{sk} showed a predominance of peaks above

the mean plane to TU and SL ($S_{sk} > 0$) implants. After insertion, the reduction on the S_{sk} values of TU and SL implants indicates a shift on the height profile towards a more symmetrical distribution explained by loss of the peaks. In contrast, S_{sk} initial negative value for OS implants reveals that the initial surface was composed predominantly by valleys and the similar values before and after insertion indicated that height distribution was not affected (Figure 4). The developed interfacial area ratio (S_{dr}) values alteration followed the same pattern as observed for S_a ; higher reduction to SL ($\Delta 23.2\%$) followed by TU ($\Delta 6.2\%$) and OS ($\Delta 2.3\%$).

TU implants exhibited slightly deeper extreme valleys (S_{vk}) after insertion coupled to a reduction of both the core roughness (S_k) and extreme peaks (S_{pk}) of $0.28 \mu\text{m}$ and $0.17 \mu\text{m}$ that resulted in an overall height reduction ($S_{vk}+S_k+S_{pk}$) of $0.33 \mu\text{m}$. OS implants exhibited a reduction of the S_{vk} and S_k of $0.12 \mu\text{m}$ and $0.22 \mu\text{m}$, where the S_{pk} was similar after insertion, resulting on an overall reduction of $0.33 \mu\text{m}$. Although the OS and SL undergo similar surface modifications, the functional parameters modification indicated a different behavior under stress. SL implants were mainly affected on the extreme peaks, with a reduction of the S_{pk} of $0.69 \mu\text{m}$, while the core roughness and extreme valleys showed a reduction of $0.45 \mu\text{m}$ and $0.22 \mu\text{m}$ that resulted in an overall height reduction of $1.36 \mu\text{m}$ (Figure 5). An example of a SL implant measurement of the same thread before and after shows that the extreme peaks were predominantly affected compared to the core roughness and extreme valleys (Figure 6).

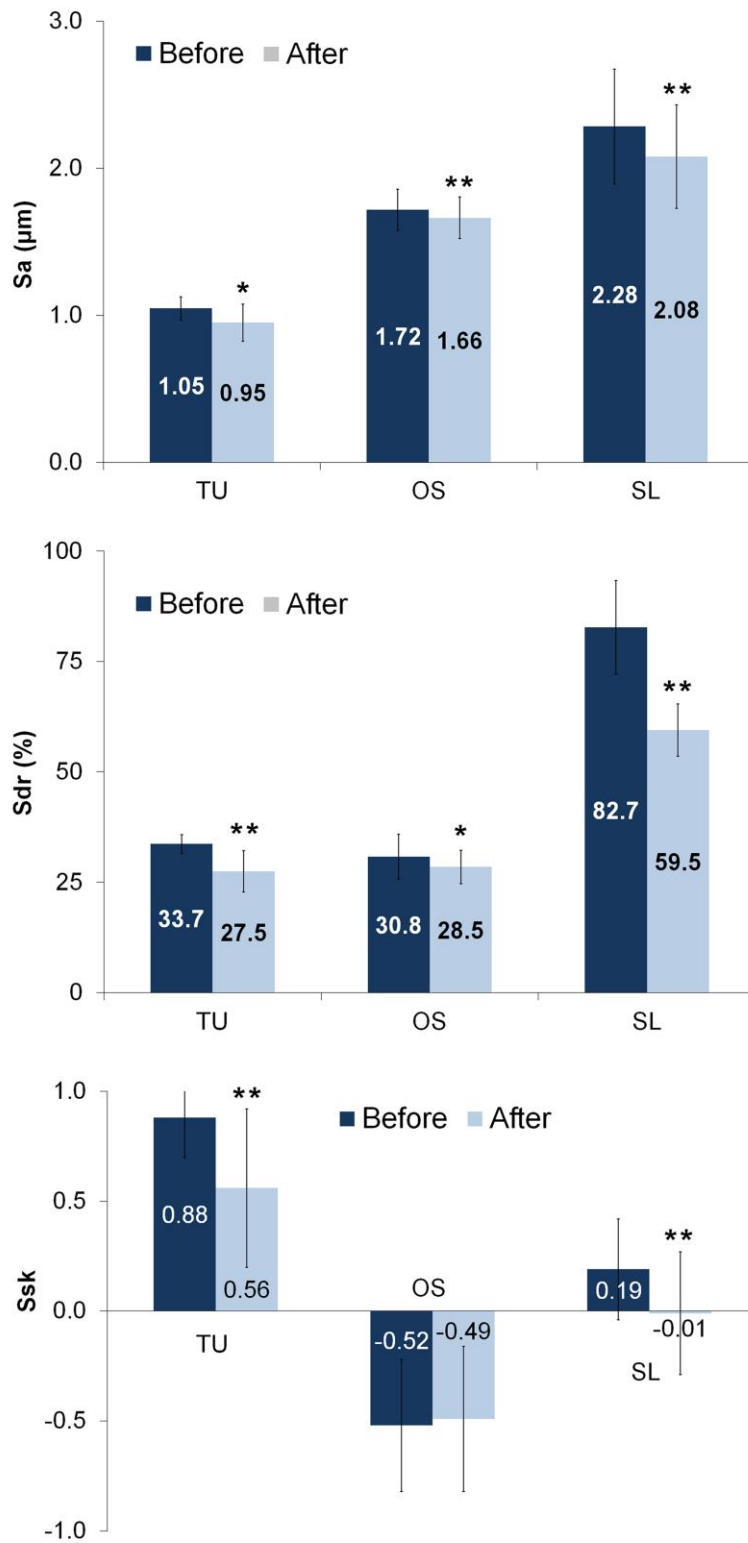


Figure 4. Surface roughness Sa, Sdr and Ssk parameters (mean and standard deviation) of the implants before and after insertion into bone (* = P < 0.05 and ** = P < 0.01).

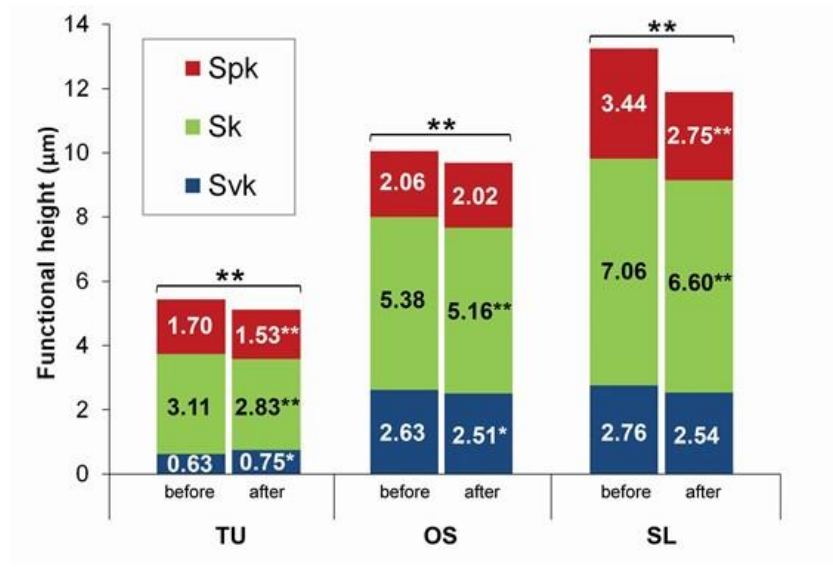


Figure 5. The surface functional height (Svk+Sk+Spk) of implants before (B) and after (A) insertion into bone (* = $P < 0.05$ and ** = $P < 0.01$).

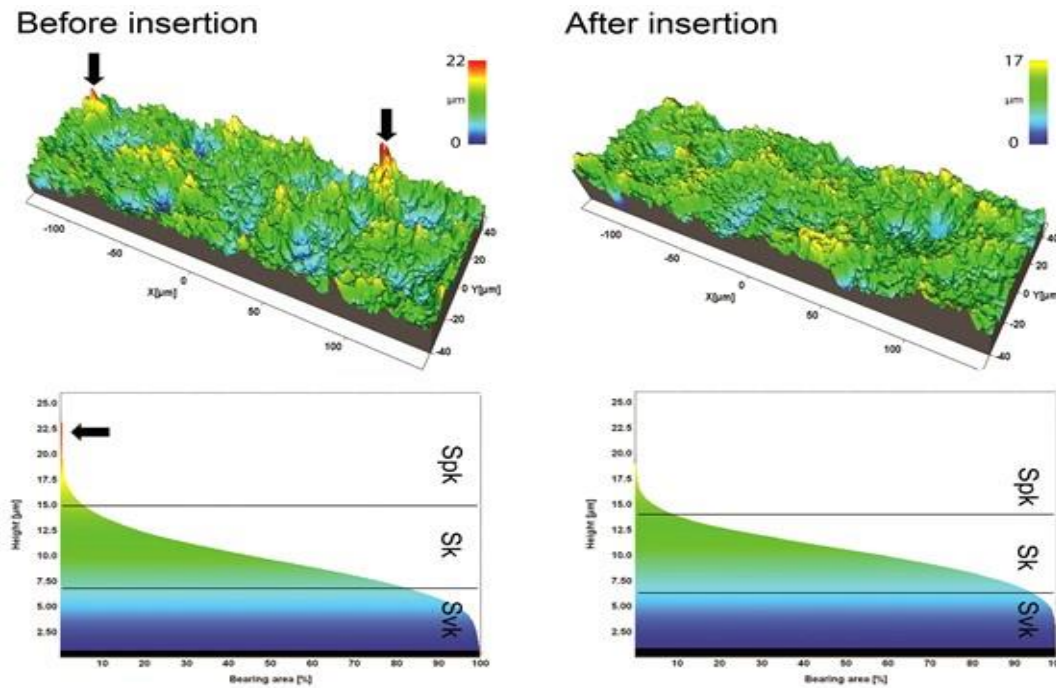


Figure 6. The surface topography of a thread of SL implants before and after insertion into bone and respective bearing area curves. Summits (red peaks) were visually less prevalent after implant insertion.

TU, OS and SL groups demonstrated an average Vm reduction of the volume at the crest of the threads of 8,723 μm^3 , 13,320 μm^3 and 31,431 μm^3 (Figure 7). This corresponded to 0.06, 0.14 and 0.54 mg of released particles from TU, OS and SL implants. The threads were randomly damaged during insertion, even in the same implant group, as observed by the broad range of Vm reduction considering each thread (Figure 8). While some threads were minimally affected, others threads of OS and SL implants exhibited the highest structural height reduction (Figure 9).

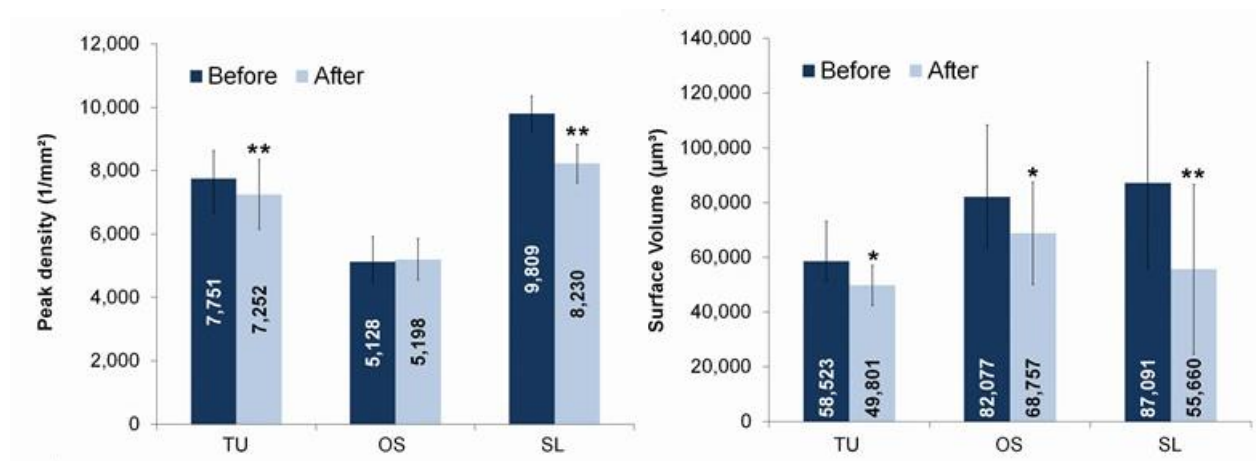


Figure 7. Peak density and surface volume (mean and standard deviation) of implants before and after insertion into bone (* = P < 0.05 and ** = P < 0.01).

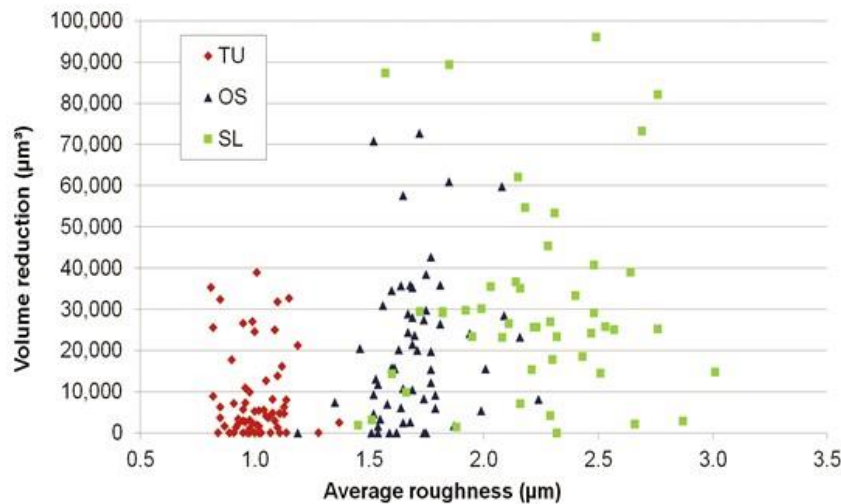


Figure 8. The surface volume reduction after implant insertion according to the average roughness (Sa) computed at the crest of all threads of TU, OS and SL groups.

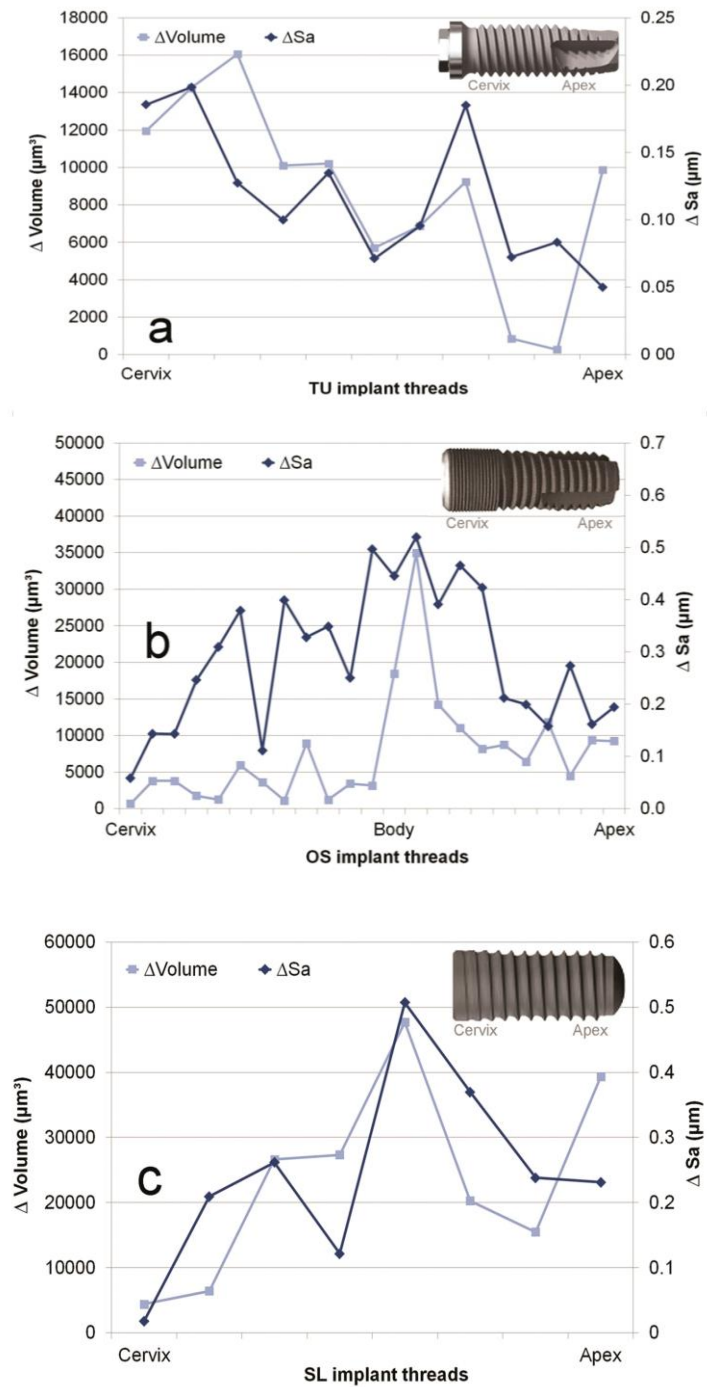


Figure 9. The average roughness (Sa) and surface volume (Vm) reduction on each individual thread after insertion along TU (a), OS (b) and SL (c) implants.

After insertion, SEM images of TU implants showed chipping of the porous structures along the surface associated with cracks on the base of the anodized layer (Figure 10a). Also, delamination was seen at the sharp edges of the cutting-threads with exposure of bulk titanium (Figure 10b). The sharp peaks present initially at the grit-blasted and acid-etched implants (OS and SL) were less prominent or completely removed after insertion, resulting in flattened smooth areas (Figure 11 and 12). The BSD/EDS evaluation revealed presence of titanium debris along the implantation site of bone blocks separated from TU, SL and OS implants (Figure 10, 11 and 12). Loose titanium particles of 10 nm to 20 μm were seen on the implantation sites, concentrated mainly around the cortical bone layer, especially at the microthreads region of OS implants. Bone blocks adjacent to SL implants revealed Al particles (Figure 13).

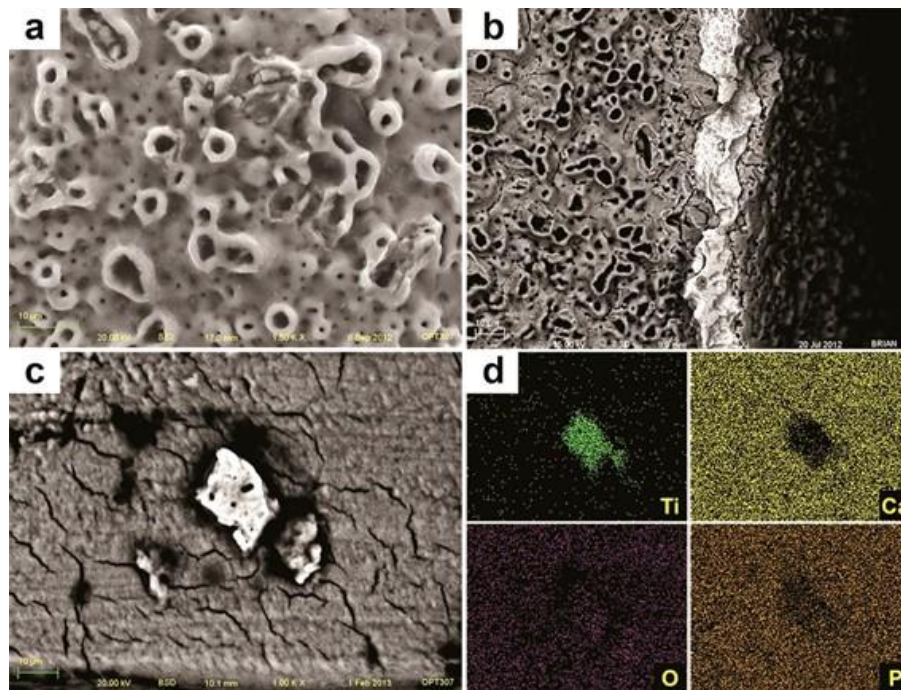


Figure 10. SEM image of TU implant after insertion into bone revealed chipping of the more extreme porous (a) and cracks on the oxide layer associated to loss of entire oxide layer at the cutting edge with exposure of the bulk Ti (b). Along the implantation sites, pieces of the oxide layer were identified by SEM-BSD (c) and their Ti content was shown by EDS mapping of the surface (d).

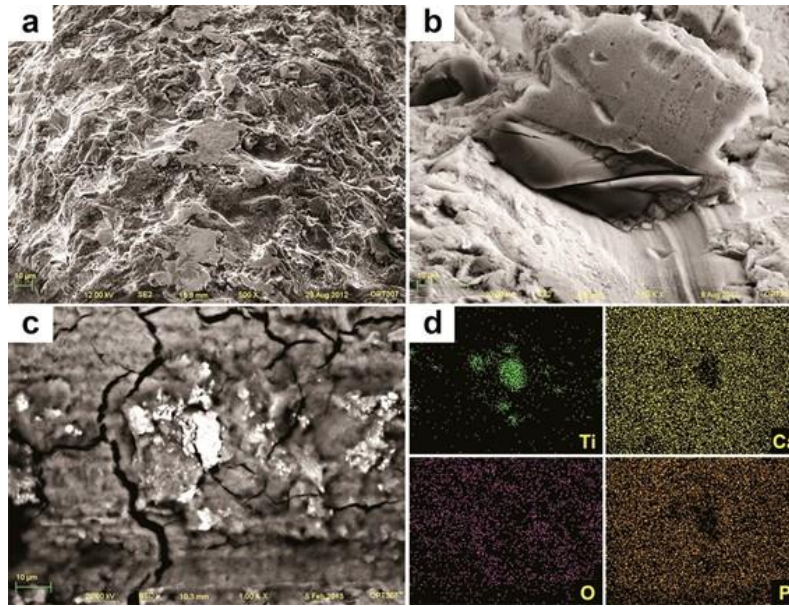


Figure 11. SEM image of OS implant after insertion into bone revealed sharp peaks less prominent or completely removed, resulting in flattened smooth areas after implant insertion (a). Also, the TiO₂ grit-particles (dark and smooth) embedded into the surface (b) were less prevalent after insertion. Along the implantation sites, particles were identified by SEM-BSD (c) and their Ti content was shown by EDS mapping of the surface (d).

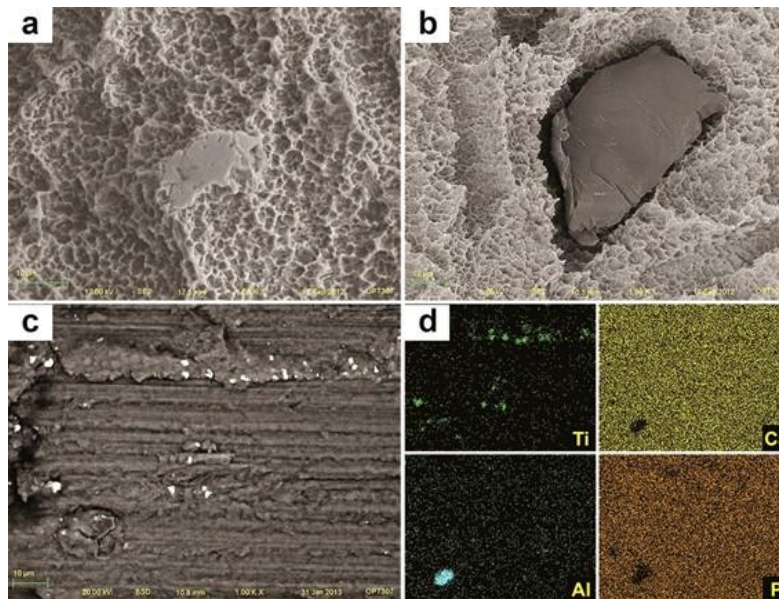


Figure 12. SEM image of SL implant after insertion into bone revealed sharp peaks less prominent or completely removed, resulting in flattened smooth areas after implant insertion (a). Also, the alumina grit-particles (dark and smooth) embedded into the surface (b) were less prevalent after insertion. Along the implantation sites, particles were identified by SEM-BSD (c) and their Ti and Al content was shown by EDS mapping of the surface (d).

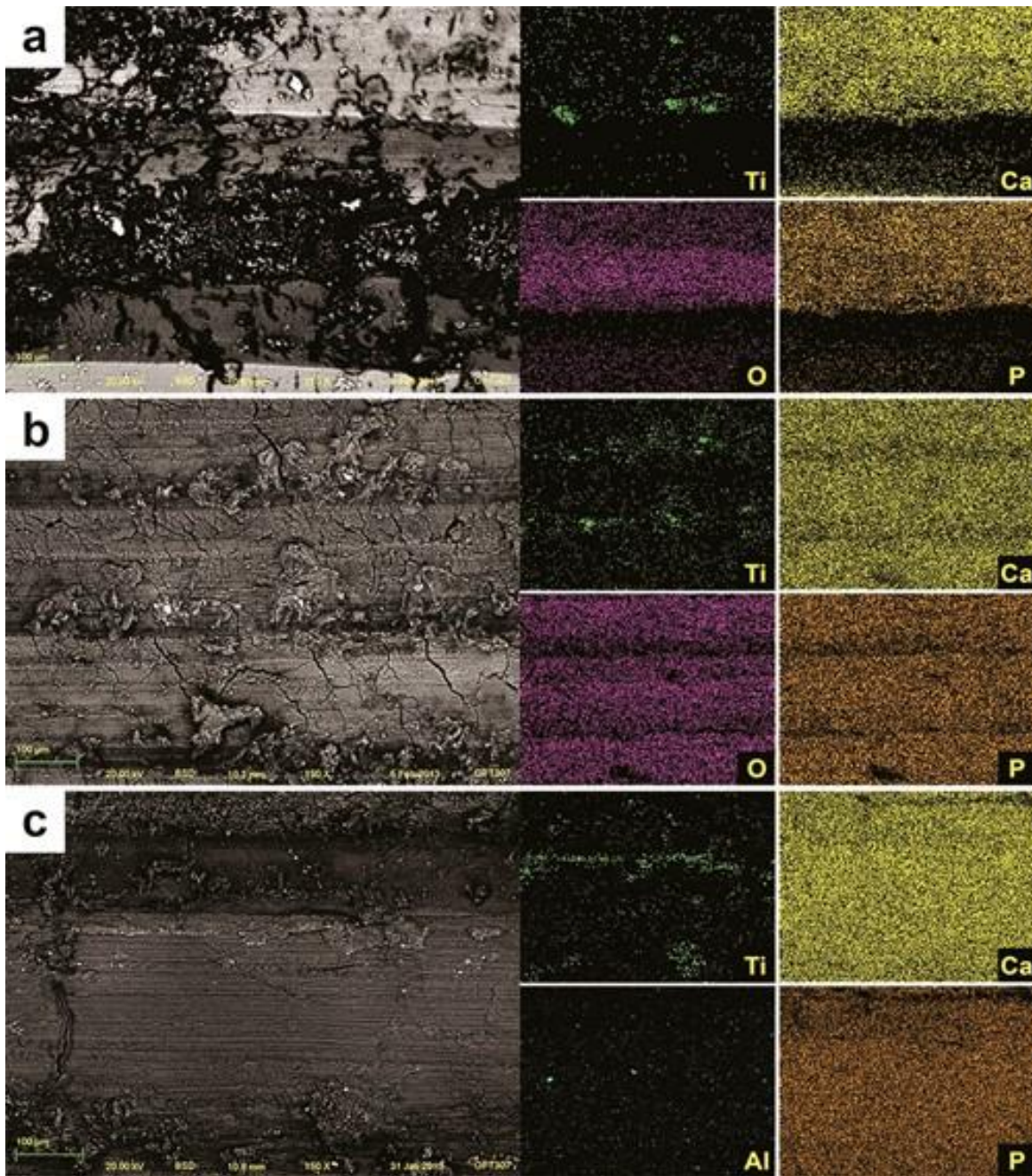


Figure 13. SEM-BSD images of the implantation sites showed titanium loose particles (white shiny spots) along all implantation sites after removal of TU (a), OS (b) and SL implants (c). The elemental content of those particles (Ti for TU and OS, and Ti and Al for SL implants) was confirmed by the EDS mapping of the surface.

DISCUSSION

Pilot tests were performed to ensure that the maximum insertion torque for the implant groups never exceeded the values recommended by each company. This critical step was important to simulate an ideal placement and to ensure that any damage to the surface was not related to implant overtorque. In addition, secondary damage was achieved by cutting the bone blocks in half prior to implant insertion, allowing an easy removal of the implant by separating the block in two pieces. It would be hard to estimate any further damage related to the attempt to remove the implant by unscrewing or cutting the bone block with the implant already installed. Thus, any change in surface topography of the implants evaluated in the present study is restricted to the actual insertion procedure and does resemble the clinical scenario.

The S_a is the most used roughness parameter used to characterize implant surfaces and indicated that the height of the structures were more affected on the rougher SL implants. The higher surface alteration to the rougher SL implant was further confirmed by the more pronounced reduction of the hybrid S_{dr} parameter and the more pronounced reduction of surface volume compared to TU and OS implants. However, it was not clear the reason why both blasted and acid-etched implants (OS and SL) experienced such clear distinguished alteration after insertion.

The amplitude and hybrid parameters demonstrated change in the surface topography of all three groups but they are not sensitive to indicate the pattern of wear within the surface. To complement the amplitude and hybrid parameters, functional parameters are an alternative to separate the features within the surface. Surface features are separated as extreme peaks (S_{pk}), core (S_k) and extreme valleys (S_{vk}), providing a tool to inspect the damage at different levels.³ This approach proved to be a valuable technique to analyze different surfaces of dental implants and identify where the damage occurred. SL rougher implant demonstrated a pronounced reduction of S_{pk} and decreased S_k after insertion, whereas the S_{vk} were not statistically different. In contrast to SL implants, OS

implants demonstrated a reduction of the core roughness (S_k) and the deep valleys (S_{vk}) while the extreme peaks were not affected (Figure 5).

SL and OS implants are treated by the same surface modification techniques (blasting and acid-etching) but the two implants have a clear different height distribution. OS implants exhibit a surface predominantly formed by structures below the mean plane ($S_{sk} < 0$), whereas the SL implants have a slight asymmetry towards structures above the mean plane ($S_{sk} > 0$), explaining the unexpected similar S_{pk} values before and after insertion for the OS implants and overall higher surface alteration to the rougher and positively skewed SL implants. The chipping of the oxide layer of the anodized TU implants at some threads explains the discrete increase of the S_{vk} , resulting in some deeper structures combined to the expected wear of the S_{pk} extreme peaks extending to the S_k core roughness. The direct analysis of the peak density values corroborated with the alterations detected by the roughness parameters. Positively skewed surfaces of TU and SL implants demonstrated a significant reduction of the number of peaks after insertion, whereas the negatively skewed OS implants revealed similar values before and after insertion (Figure 7). It is clear from the present results that the negative height distribution associated to a lower S_{dr} reduced the overall modification of the OS implants despite the higher S_a value compared to TU implants and the combination of higher S_a and S_{dr} values associated to a positive height distribution on SL implants determine the more pronounced volume reduction.

The present study showed that the insertion procedure itself is able to release up to 0.5 mg of particles at implant-bone interface. Previous studies reported that titanium particle-induced osteolysis can be initiated from approximately 0.2 mg 24 to 3.0 mg 25 of loose titanium particles, showing extensive and non-uniform osteoclastic activity with a resorbed bone area 8% 24 to 35% 25 higher than the control sites without particles. This same pattern of osteolysis was identified in face of higher quantity of particles: 20 mg 26 and 30 mg.²⁷⁻²⁹

In contrast, Goodman et al.¹⁸ reported that approximately 113 mg to 1.13 g of titanium particles did not affect the bone remodeling process in vivo. However, the bone tissue was evaluated after 16 weeks of the introduction of the particles. Since the osteolytic response to titanium particles seems to be transient and rapidly repaired in young and healthy mice, with the peak of bone resorption after 7 days and returning to baseline levels by 13 days,²⁴ this period of 16 weeks allowed the evaluation after the osteolysis took place. Indeed, after 12 to 24 weeks, it was showed presence of titanium particles in the regional lymph nodes after insertion of implants in the jaws of sheep,³⁰ mini pigs 5 and beagle dogs,³¹ as well as in the liver, lungs and kidneys.⁵ This indicates the possibility of migration of these particles released from the surface of dental implants from the jaw bone to other organs.

Future studies should evaluate the physiological response to titanium particles-induced osteolysis considering the implant design and surface topography, and surgical technique which can vary the quantity, size and chemical constituent of the particles. Moreover, the modulation of this process by the subject healthy status should be investigated.

CONCLUSION

Surface damage was observed on all three implant groups. The combined enhanced Sa and positive Ssk values of SL implants resulted in more surface damage during the insertion procedure. Loose titanium particles of different sizes were detected embedded in the bone walls as a result of wear of the surface features. Future experiments should elucidate the clinical relevance of such particles on peri-implant tissues response.

ACKNOWLEDGMENTS

This work was supported by National Institutes of Health PHS award P30 AR61307. The authors would like to thank to the São Paulo Research Foundation (FAPESP #2011/23269-0) for the scholarship granted to the first author.

REFERENCES

1. Elias CN, Meirelles L. Improving osseointegration of dental implants. *Expert Rev Med Devices* 2010; 7:241-256.
2. Wennerberg A, Albrektsson T, Ulrich H, Krol JJ. An Optical 3-Dimensional Technique for Topographical Descriptions of Surgical Implants. *Journal of Biomedical Engineering* 1992; 14:412-418.
3. Dong WP, Stout KJ. An Integrated Approach to the Characterization of Surface Wear .1. Qualitative Characterization. *Wear* 1995; 181:700-716.
4. Wennerberg A, Albrektsson T, Andersson B. An Animal Study of Cp Titanium Screws with Different Surface Topographies. *Journal of Materials Science-Materials in Medicine* 1995; 6:302-309.
5. Schliephake H, Reiss G, Urban R, Neukam FW, Guckel S. Metal release from titanium fixtures during placement in the mandible: an experimental study. *Int J Oral Maxillofac Implants* 1993; 8:502-511.
6. Meyer U, Buhner M, Buchter A, Kruse-Losler B, Stamm T, Wiesmann HP. Fast element mapping of titanium wear around implants of different surface structures. *Clin Oral Implants Res* 2006; 17:206-211.
7. Martini D, Fini M, Franchi M, Pasquale VD, Bacchelli B, Gamberini M, Tinti A, Taddei P, Giavaresi G, Ottani V, Raspanti M, Guizzardi S, Ruggeri A. Detachment of titanium and fluorohydroxyapatite particles in unloaded endosseous implants. *Biomaterials* 2003; 24:1309-1316.
8. Franchi M, Bacchelli B, Martini D, Pasquale VD, Orsini E, Ottani V, Fini M, Giavaresi G, Giardino R, Ruggeri A. Early detachment of titanium particles from various different surfaces of endosseous dental implants. *Biomaterials* 2004; 25:2239-2246.
9. Franchi M, Orsini E, Martini D, Ottani V, Fini M, Giavaresi G, Giardino R, Ruggeri A. Destination of titanium particles detached from titanium plasma sprayed implants. *Micron* 2007; 38:618-625.
10. Flatebo RS, Hol PJ, Leknes KN, Kosler J, Lie SA, Gjerdet NR. Mapping of titanium particles in peri-implant oral mucosa by laser ablation inductively coupled

plasma mass spectrometry and high-resolution optical darkfield microscopy. *J Oral Pathol Med* 2011; 40:412-420.

11. Flatebo RS, Johannessen AC, Gronningsaeter AG, Boe OE, Gjerdet NR, Grung B, Leknes KN. Host response to titanium dental implant placement evaluated in a human oral model. *J Periodontol* 2006; 77:1201-1210.

12. Goodman SB, Trindade M, Ma T, Genovese M, Smith RL. Pharmacologic modulation of periprosthetic osteolysis. *Clin Orthop Relat Res* 2005:39-45.

13. Tuan RS, Lee FY, Y TK, Wilkinson JM, Smith RL. What are the local and systemic biologic reactions and mediators to wear debris, and what host factors determine or modulate the biologic response to wear particles? *J Am Acad Orthop Surg* 2008; 16 Suppl 1:S42-48.

14. Bukata SV, Gelinas J, Wei X, Rosier RN, Puzas JE, Zhang X, Schwarz EM, Song XY, Griswold DE, O'Keefe RJ. PGE2 and IL-6 production by fibroblasts in response to titanium wear debris particles is mediated through a Cox-2 dependent pathway. *J Orthop Res* 2004; 22:6-12.

15. Wang JY, Wicklund BH, Gustilo RB, Tsukayama DT. Titanium, chromium and cobalt ions modulate the release of bone-associated cytokines by human monocytes/macrophages in vitro. *Biomaterials* 1996; 17:2233-2240.

16. Goodman SB, Ma T. Cellular chemotaxis induced by wear particles from joint replacements. *Biomaterials* 2010; 31:5045-5050.

17. Schwarz EM, Benz EB, Lu AP, Goater JJ, Mollano AV, Rosier RN, Puzas JE, Okeefe RJ. Quantitative small-animal surrogate to evaluate drug efficacy in preventing wear debris-induced osteolysis. *J Orthop Res* 2000; 18:849-855.

18. Goodman SB, Davidson JA, Song Y, Martial N, Fornasier VL. Histomorphological reaction of bone to different concentrations of phagocytosable particles of high-density polyethylene and Ti-6Al-4V alloy in vivo. *Biomaterials* 1996; 17:1943-1947.

19. Buly RL, Huo MH, Salvati E, Brien W, Bansal M. Titanium wear debris in failed cemented total hip arthroplasty. An analysis of 71 cases. *J Arthroplasty* 1992; 7:315-323.

20. Kadoya Y, Revell PA, al-Saffar N, Kobayashi A, Scott G, Freeman MA. Bone formation and bone resorption in failed total joint arthroplasties: histomorphometric analysis with histochemical and immunohistochemical technique. *J Orthop Res* 1996; 14:473-482.
21. Guan H, Staden RCv, Johnson NW, Loo Y-C. Dynamic modelling and simulation of dental implant insertion process-A finite element study. *Finite Elem. Anal. Des.* 2011; 47:886-897.
22. Katranji A, Misch K, Wang HL. Cortical bone thickness in dentate and edentulous human cadavers. *J Periodontol* 2007; 78:874-878.
23. Wennerberg A, Albrektsson T. On implant surfaces: a review of current knowledge and opinions. *Int J Oral Maxillofac Implants* 2010; 25:63-74.
24. Kaar SG, Ragab AA, Kaye SJ, Kilic BA, Jinno T, Goldberg VM, Bi Y, Stewart MC, Carter JR, Greenfield EM. Rapid repair of titanium particle-induced osteolysis is dramatically reduced in aged mice. *J Orthop Res* 2001; 19:171-178.
25. Shin DK, Kim MH, Lee SH, Kim TH, Kim SY. Inhibitory effects of luteolin on titanium particle-induced osteolysis in a mouse model. *Acta Biomater* 2012; 8:3524-3531.
26. Tsutsumi R, Hock C, Bechtold CD, Proulx ST, Bukata SV, Ito H, Awad HA, Nakamura T, O'Keefe RJ, Schwarz EM. Differential effects of biologic versus bisphosphonate inhibition of wear debris-induced osteolysis assessed by longitudinal micro-CT. *J Orthop Res* 2008; 26:1340-1346.
27. Darowish M, Rahman R, Li P, Bukata SV, Gelinas J, Huang W, Flick LM, Schwarz EM, O'Keefe RJ. Reduction of particle-induced osteolysis by interleukin-6 involves anti-inflammatory effect and inhibition of early osteoclast precursor differentiation. *Bone* 2009; 45:661-668.
28. Childs LM, Goater JJ, O'Keefe RJ, Schwarz EM. Effect of anti-tumor necrosis factor-alpha gene therapy on wear debris-induced osteolysis. *J Bone Joint Surg Am* 2001; 83-A:1789-1797.

29. Jin S, Park JY, Hong JM, Kim TH, Shin HI, Park EK, Kim SY. Inhibitory effect of (-)-epigallocatechin gallate on titanium particle-induced TNF-alpha release and in vivo osteolysis. *Exp Mol Med* 2011; 43:411-418.
30. Frisken KW, Dandie GW, Lugowski S, Jordan G. A study of titanium release into body organs following the insertion of single threaded screw implants into the mandibles of sheep. *Aust Dent J* 2002; 47:214-217.
31. Weingart D, Steinemann S, Schilli W, Strub JR, Hellerich U, Assenmacher J, Simpson J. Titanium deposition in regional lymph nodes after insertion of titanium screw implants in maxillofacial region. *Int J Oral Maxillofac Surg* 1994; 23:450-452.

Capítulo 2:

Early cell response to titanium surface nitrided by plasma ion immersion technique

Plinio Senna;^a Cindy Goes Dodo;^a Yuri Wanderlei Cavalcanti;^a Carlos Salles Lambert;^b Karina Gonzales Silvério Ruiz;^a Altair A. Del Bel Cury.^a

^a Department of Prosthodontics and Periodontology, Piracicaba Dental School, State University of Campinas, Brazil.

^b Institute of Physics Gleb Wataghin, State University of Campinas, Campinas, Brazil.

Corresponding author:

Altair Antoninha Del Bel Cury

Department of Prosthodontics and Periodontology, Piracicaba Dental School, State University of Campinas. Avenida Limeira, 901. Zip Code: 13414-903. Piracicaba, São Paulo, Brazil.

Phone: +55 19 21065294; Fax +55 19 2106-5211;

ABSTRACT

The aim of this study was to evaluate the effect of nitrided Ti surface obtained by plasma ion implantation technique on the initial cell response using human osteoblast cells. For this, titanium grade 4 discs (12.7×2 mm) were blasted by aluminum oxide particles to produce moderately rough surfaces (Ti). After cleaning, the experimental discs (TiN) were placed inside a vacuum chamber to be nitrided by plasma ion implantation technique. Roughness was characterized by laser confocal microscopy and atomic force microscopy. In addition, the chemical profile and Knoop hardness were evaluated. Surface energy was determined by measuring the contact angle of a sessile drop by a goniometer. To evaluate the biocompatibility of the surface, human osteoblasts (SAOS-2) were seeded on the discs (2×10^4 cells) and cultured for 1, 3, 5 and 7 days. To evaluate cell attachment and proliferation, MTS was added to each well and the absorbance read at 490 nm after 4 h of incubation. At day 7, alkaline phosphatase (ALP) activity was measured to evaluate differentiation using a commercial kit to detect the release of thymolphthalein and quantitative real-time polymerase chain reaction (qPCR) was used to evaluate gene expression of osteoblast markers. In addition, cell morphology was determined by SEM and confocal laser scanning microscopy. TiN group exhibited similar micro-roughness than Ti group; however, there was more nanostructures, higher nitrogen content and hardness, and slight better wettability. Despite the surface changes, similar cell proliferation and differentiation was identified after 7 days of culture. It was possible to conclude that nitrogen plasma increased the surface hardness and the presence of nanostructures and did not jeopardize titanium biocompatibility.

Keywords: titanium; nitriding; cell culture; osseointegration.

INTRODUCTION

Physical and chemical treatments have been proposed to create rough surfaces on dental implants to improve initial bone formation and bone support over time.¹ Thus, the majority of modern dental implant surfaces present surface features with 1 to 2 μm average height deviation.² These peaks on surface may be prone to break and detach during the insertion procedure since titanium has low abrasion resistance.³ Indeed, previous studies detected loose titanium particles in the connective tissue adjacent to the implant surface.^{4, 5}

Plasma immersion ion implantation is a surface treatment commonly used to improve wear and corrosion resistance of stainless steel and aluminum alloys and can be applied to titanium.⁶ When using nitrogen ion, titanium oxide is substituted by titanium nitride without presenting the mechanical instabilities associated to any additive surface treatments.⁷ Moreover, nitrided titanium showed to present higher surface hardness without affecting titanium biocompatibility.^{7, 8} Thus, with the potential to reduce wear, plasma nitriding may be used to reduce titanium debris generation and to minimize bone loss over time.

Different plasma immersion techniques has been used to modify the surface of biomaterials.⁹ With the hollow cathode technique, higher cell adhesion was reported and slightly favored osteoblast differentiation.^{9, 10} However, it can be consequence of the increase on roughness caused by this technique,⁹ which can favor cell response by the presence of more nanostructures on titanium.¹¹ However, there is a lack of information about the biocompatibility of other plasma techniques. Therefore, the aim of this study was to evaluate the effect of nitrided Ti surface obtained by plasma ion implantation technique on the initial cell response using human osteoblast cells.

MATERIALS AND METHODS

Titanium discs

Titanium discs ($12.7 \times 2 \text{ mm}$) were fabricated from a bar of commercially pure grade 4 titanium (Sandinox, Sorocaba, SP, Brazil). The surface was blasted

by aluminum oxide particles with 150 μm diameter. The discs were washed in ultrasonic bath for 20 min in acetone, ethanol and purified water, and dried under vacuum (Ti - control group). The experimental discs (TiN) were placed inside a vacuum chamber (10^{-8} torr) to be nitrided by plasma ion implantation technique.⁶ First, surface sputtering by argon ions (3 kV) were used to remove contaminants and clean the discs. After, nitrogen plasma is created with increased electrical potential difference to nitride the surface. After, all discs were sterilized by 25 kGy gamma radiation (CBE Embrarad, Jarinu, SP, Brazil).

The surface roughness was characterized using laser confocal microscopy (Lext OLS4000; Olympus Corporation, Tokyo, Japan) to compute the average height deviation (S_a) and the increased area ratio (S_{dr}). Atomic force microscopy (Dimension Edge, Veeco Billerica, MA, USA) using a 125 nm cantilever silicon probe (Digital Instruments, Santa Bárbara, EUA) in tapping mode was used to detect nanostructures. The images were processed with a third-order least-squares fit correction to remove errors of tilt and bow (SPIP software v.5.8; Image Metrology A/S, Hørsholm, Denmark). The chemical profile was detected on XPS spectrums (VSW HA-100; VSW Atomtech, Oxfordshire, UK) and hardness was performed with a microhardness tester (Shimadzu HMV-2000, Kyoto, Japan), using a Knoop indenter with a 10 g load for 5 s. Five indentations were made on each specimen at a distance of 100 μm between them and the average was considered the microhardness value for the specimen.

Surface wettability was determined by contact angle of a sessile drop (15 μL) of purified water dispensed on the surface. The contacting angle at air-liquid-disc intersection was recorded and measured using a goniometer (ramé-Hart 500 advanced; Ramé-hart Instrument Co., Succasunna, NJ, USA). In addition, the surface energy was determined using the Lifshitz–van der Waals/acid-base method,¹² in which the cosine of the contact angle of water and two extra liquids: bromonaphthalene and formamide (Sigma-Aldrich Corp., St. Louis, MO, USA) were used.¹³

Cell response analysis

Human osteoblast cells (SAOS-2; ATCC, VA, USA) were used to determine cell proliferation and differentiation. Cells were propagated in McCoy 5A medium supplemented with 15% fetal bovine serum and 1% penicillin-streptomycin (Pen Strep; Gibco Life Technologies, NY, USA). Freshly fed subconfluent cells were harvested and 2×10^4 cells were let to adhere on the surface of the discs placed in 24-well tissue plates (TPP, Switzerland). After 3 h of incubation, the non-adherent cells were washed away by three gentle changes of medium.

Cell proliferation was evaluated after 1, 3, 5 and 7 days of incubation. After each time point, the discs were washed by medium change and a tetrazolium compound was added to each well (CellTiter 96® AQueous One Solution Cell Proliferation (MTS); Promega, WI, USA). After 4 h of incubation at 37°C, all medium was collected and an aliquot of 100 µl was used to read the absorbance at 490 nm (Multiskan Spectrum Microplate Spectrophotometer, Thermo Fisher Scientific Inc., MA, USA). Six disks from each group were measured at each time point.

At day 7, alkaline phosphatase (ALP) activity was measured to evaluate differentiation using a commercial kit (Labtest Diagnostica SA, Belo Horizonte, MG, Brazil), which detects the release of thymolphthalein from thymolphthalein monophosphate. The cells were collected after trypsin-EDTA treatment and resuspended in 1 ml of DPBS to be lysed by ultrasound (7 W/ 2 min). After, 50 µl of cell lysates were added to the kit and the absorbance was measured at 590 nm. ALP activity was expressed as U/L. Six disks from each group were measured.

In addition, quantitative real-time polymerase chain reaction (RT-PCR) was used after 7 days of culture to evaluate the gene expression of runt-related transcription factor 2 (Runx-2), ALP. Osteopontin (OPN), osteocalcin (OC) and bone morphogenetic protein 2 (BMP-2). The gene expression of the enzyme glyceraldehyde 3-phosphate dehydrogenase (GAPDH) was used as reference. The total RNA was extracted with Trizol reagent (Invitrogen, Life Technologies, USA) according to the manufacturer's instructions and purified after DNase I treatment (Invitrogen, USA). The concentration and purity of RNA samples was determined by

optical density (Nanodrop, Thermo Fischer Scientific, USA). After, complementary DNA (cDNA) was synthesized from 1 µg of purified RNA using a reverse transcription reaction (iScript™ cDNA Synthesis Kit, Bio-Rad Laboratories, CA, USA). Real-time PCR was carried out in the MniOpticon™ Real-Time PCR detection system (Bio-Rad Laboratories) using sybr green dye (iQ™ SYBR® Green Supermix, Bio-Rad Laboratories, USA) and the specific primers. Three disks from each group were used and gene expression was quantified using a cDNA gradient curve of the GAPDH gene.

Microscopy analysis

After 7 days of culture, the cells were washed by medium change, fixed using paraformaldehyde 4% for 10 minutes, permeabilized with 0.1% triton X-100 in PBS and washed. Next, the cells were serially dehydrated in alcohol to be visualized by scanning electron microscopy (model JSM 5600LV; JEOL, Peabody, MA, USA)

To be evaluated by confocal laser scanning microscopy (TCS SP5; Leica Microsystems CMS GmbH, Mannheim, German), after washing with PBS, the cells were stained with 1:200 Alexa Fluor 488 phalloidin (Molecular Probes®, Life Technologies, USA) in PBS for 1 hours and 1:200 1,5-bis[[2-(dimethylamino)ethyl]amino]-4,8-dihydroxyanthracene-9,10-dione (DRAQ5, Cell Signalling Technology, MA, USA) for 10 min. The acquired images were processed using Adobe Photoshop software (Adobe Systems, CA, USA).

Statistical analysis

After checking normality by the Kolmogorov-Smirnov test, the surfaces were compared by the *t* test with a significance level fixed at 5% (SPSS Statistics 20; IBM Corporation, Armonk, New York, USA).

RESULTS

The surface of both discs can be seen in Figure 1. Micro roughness analyses showed similar Sa and Sdr values of $1,00 \pm 0,04 \mu\text{m}$ and $34,2 \pm 2,7 \%$ for

Ti discs and $0,99 \pm 0,04 \mu\text{m}$ and $34,4 \pm 1,7 \%$ for TiN discs, respectively ($p > 0.05$). However, in the atomic force microscopy analysis, TiN surface exhibited more nanostructures than Ti surface (Figure 2).

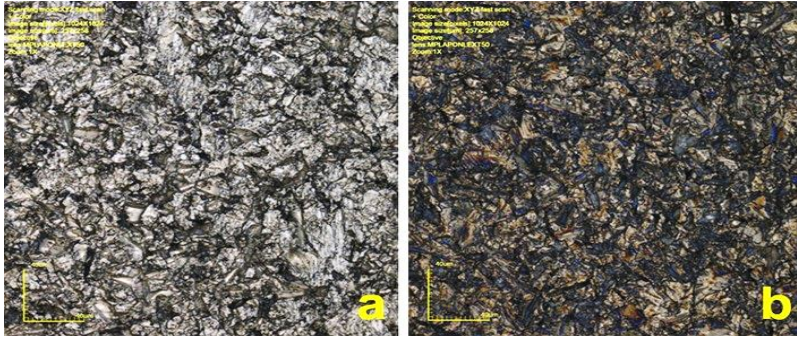


Fig 1. The surface of Ti (a) and TiN discs (b) exhibited similar roughness values despite de golden aspect of TiN surface.

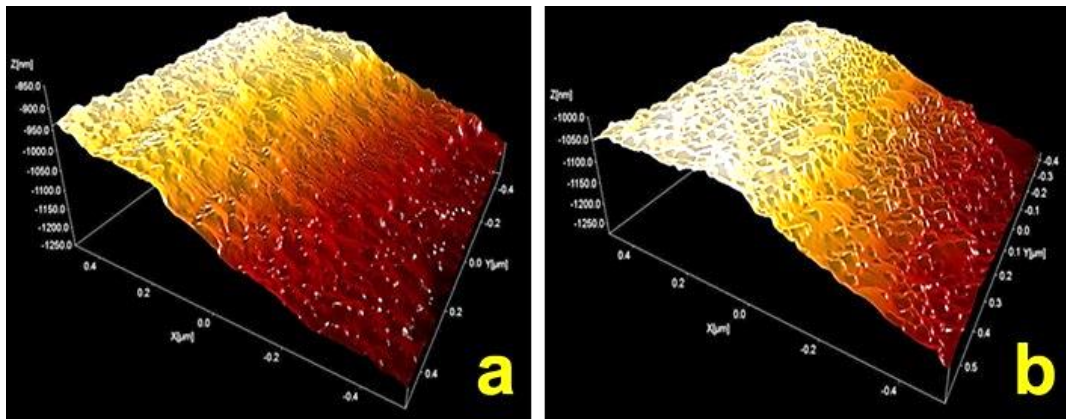


Figure 2. AFM images of Ti (a) and TiN (b) discs exhibiting an average height of the surface features (S_a) of 28.0 nm and 41.9 nm, respectively.

XPS spectrums revealed a higher content of nitrogen (400 eV) in TiN surface (Figure 3), despite small amounts of aluminum and silicon from reminiscent grit particles embedded on both surface. Knoop hardness of 441.6 ± 15.1 and $474.4 \pm 7.5 \text{ kg/mm}^2$ was identified to Ti and TiN discs, respectively ($p < 0.05$). Moreover, TiN surface exhibited slight better wettability with higher polar interaction (Table 1)

Table 1. Wettability and surface energy of Ti and TiN surfaces (mean \pm s.d.).

	Water contact angle	Surface energy		
		Polar component	Dispersive component	Total energy
TiN	75,67 \pm 3,10° *	10,42 \pm 5,04 *	25,15 \pm 2,85	32,03 \pm 2,31
Ti	80,45 \pm 4,65°	6,35 \pm 5,06	26,30 \pm 1,26	31,13 \pm 2,96

* Indicates significant different between the surfaces ($p < 0.05$, t test).

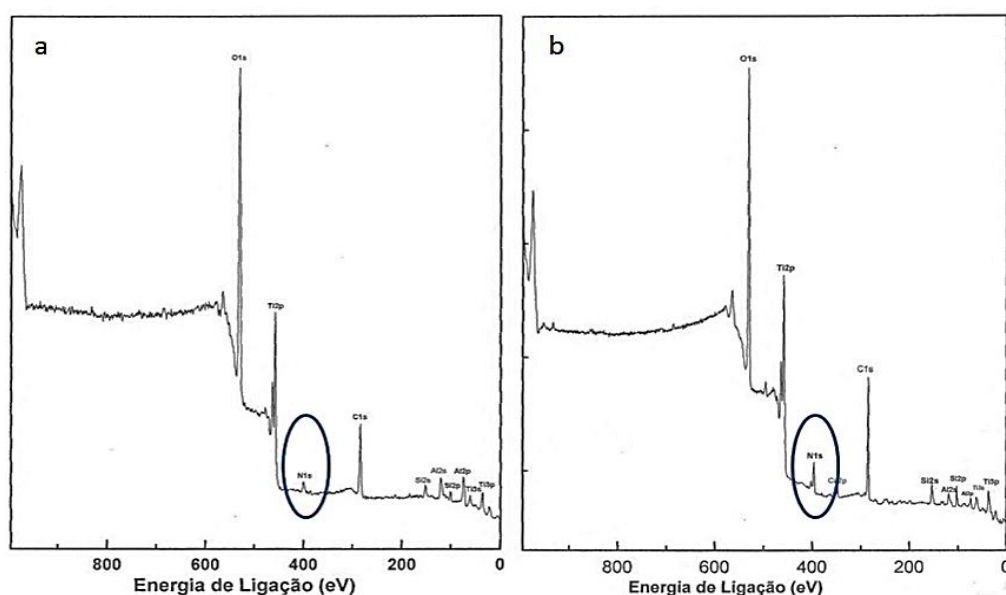


Figure 3. XPS diffractograms of Ti (a) and TiN (b) surfaces.

Cell analyzes revealed similar cell attachment and proliferation after 7 days of culture (Figure 4). Both cells presented same stage of differentiation with a low production of ALP (Figure 5) and similar expression of osteoblastic phenotype genes (Table 2).

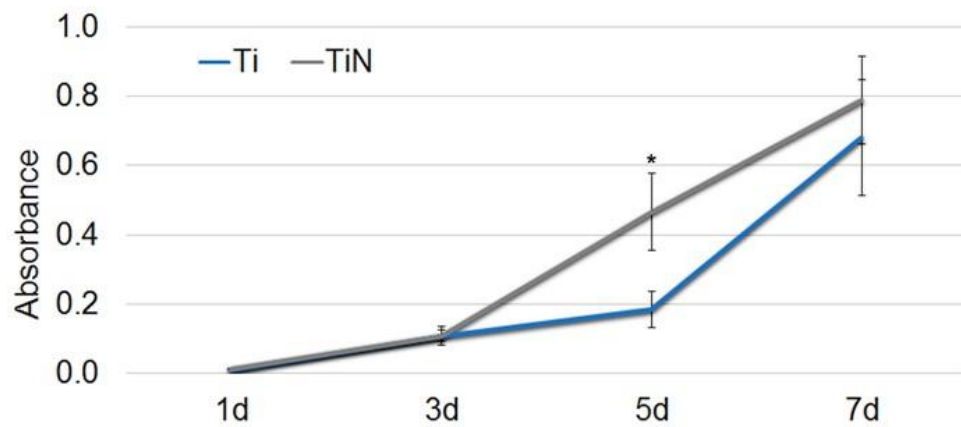


Figure 4. Cell proliferation after 1, 3, 5 and 7 days of culture.
 * Indicates significant different between the surfaces ($p < 0.05$, t test).

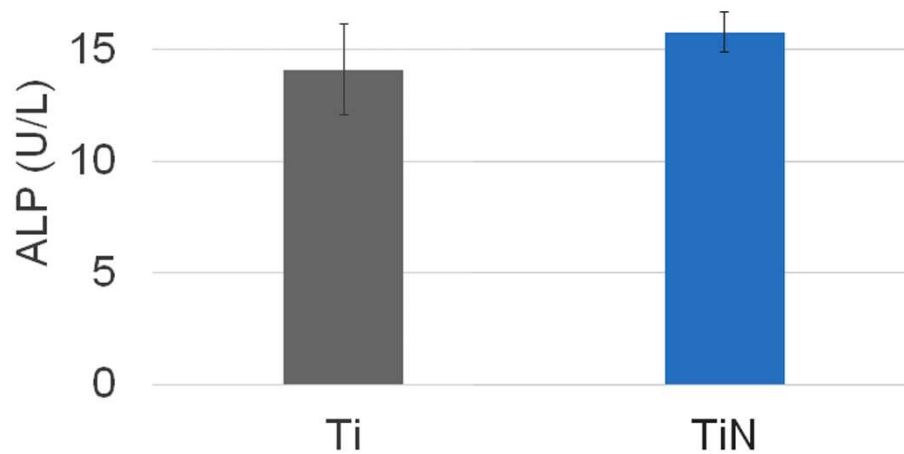


Figure 5. Alkaline phosphatase levels after 7 days of culture of SAOS-2 cells on Ti and TiN discs. No significant difference was seen ($p > 0.05$, t test).

Table 2. RNA expression (ng $\times 10^{-3}$) of cells cultured on Ti and TiN discs (mean \pm s.d.).

Gene	Groups	
	Ti	TiN
GAPDH	3.3 \pm 0.6	2.7 \pm 0.1
RUNX-2	39.4 \pm 10.4	42.1 \pm 8.3
OPN	43.2 \pm 8.1	42.1 \pm 12.3
OC	3.7 \pm 1.8	1.7 \pm 0.5 *
BMP-2	4.1 \pm 1.9	2.2 \pm 0.2 *

GAPDH = glyceraldehyde 3-phosphate dehydrogenase; RUNX-2 = runt-related transcription factor 2; OPN = Osteopontine; OC = osteocalcin; BMP-2 = bone morphogenetic protein type 2.

* Indicates significant difference between the groups ($p < 0.05$, t test).

Microscopy images revealed lamellipodia and filopodia among the SAOS-2 cells adhered on both surfaces (Figure 6). Also, similar cell density was identified on both groups (Figure 7).

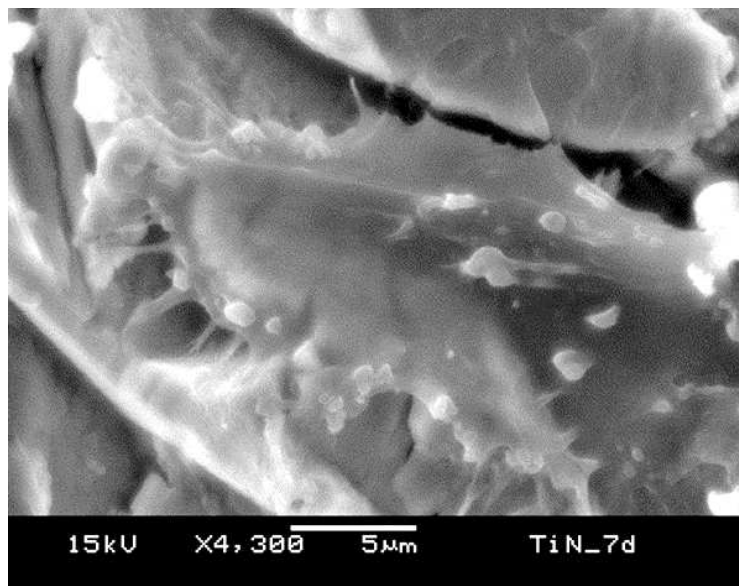


Figure 6. SEM revealed dendritic projections and small filopodia in SAOS-2 cells adhered on both surfaces.

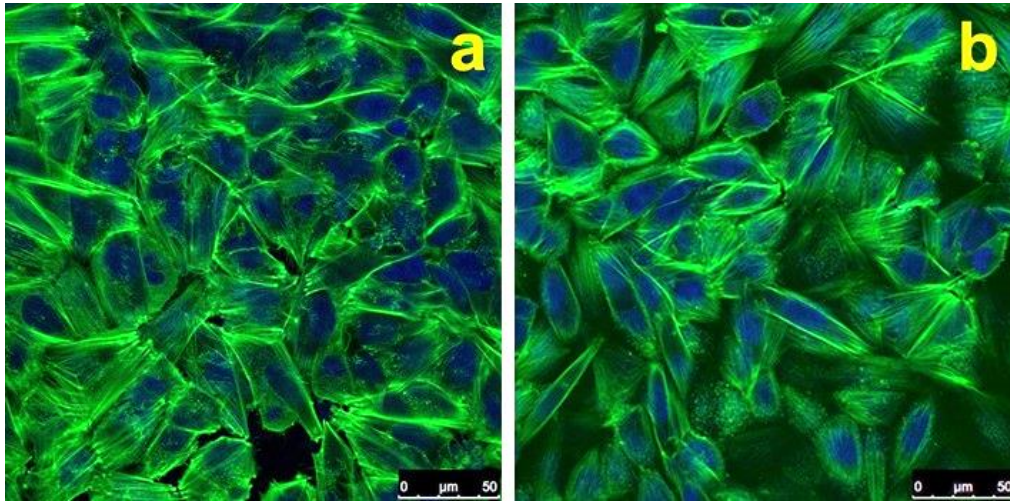


Figure 7. Confocal images showed similar distribution of cells on Ti (a) and Tin (b) discs. In green is the actin stained by phalloidin (indicating filopodia) and in blue is the core stained by the DRAQ5 dye.

DISCUSSION

The initial bone healing immediately after implant placement could be affected by the presence of loose particles that stimulate the production of pro-inflammatory cytokines by macrophages and have been associated with bone loss.¹⁴⁻¹⁶ Indeed, loose particles released from orthopedic load bearing devices due to wear triggering a chronic inflammatory and foreign body granulomatous reaction with osteolysis.^{17, 18} Thus, the present study showed that nitriding treatment, used to increase surface hardness, could be used without jeopardizing titanium biocompatibility.

This physical treatment is environmental cleanliness, low treatment temperature, short treatment time, better control, uniformity of layer thickness, and lower cost when compared to other chemical treatments.⁹ In addition, in the present study plasma nitriding on surface topography was limited to increase the density of nano-structures. However, it is not clear at this moment how the number or size of nanostructures will affect bone formation.⁶

Different ions and methods have been tested to implement nitrogen on surface. Previous studies involving cell cultures demonstrated that nitriding

treatment could enhance cell response.^{9, 10} However, when evaluating bone response *in vivo* contrasting results were identified. While one study reported that the presence of nitrogen had positive effects,¹⁹ it did not affect bone response after 3 months of healing.²⁰ However, in the present study, no significant difference of cell attachment and proliferation was seen between the groups at the time length studied. Moreover, similar patterns of cell morphology were identified on the nitrided and control titanium surfaces. These findings indicate that nitrided layer is not toxic to the cells.²¹

In general, hydrophilic surfaces would offer better conditions for cell adhesion than hydrophobic surfaces. In the present study, the ion implantation technique produced a surface with slight better wettability that did not reflect on better cell adhesion. This is in contrast to a previous study, which used the cathodic cage technique to nitride titanium and showed better wettability and cell adhesion on the nitrided surface.⁹ This controversy may corroborates that surface topography is more important to cell adhesion than the material wettability.²²

It is important to achieve a fine balance between cell proliferation and differentiation for an adequate tissue response.¹⁰ To track the differentiation of cells in the present study, it was evaluated the ALP activity and the gene expression of key osteoblast markers. Usually the ALP activity increased over time; however, in the present study, it was evaluated at only one time point and showed no difference between de groups.

The results of qPCR, showing a lower production of the late markers of osteoblast differentiation: osteocalcin and BMP-2, may indicate that the TiN surface could anticipate the turnover point, especially when the higher cell proliferation at day 5 was seen at the MTS proliferation assay. Thus, the lower expression of these genes at day 7, may indicate that a peak of expression happened earlier compaед to the Ti group. Moreover, the expression of Runx-2, which is the master regulator of osteoblast differentiation, was high on both groups, indicating that cells were not differentiated yet.

Attention is given to the surface characteristics to determine which properties would affect osseointegration. In this way, the nitriding treatment by plasma ion immersion would be one interesting to avoid release of loose titanium particles during implant insertion into bone.

CONCLUSION

Nitriding by plasma ion immersion increased the surface hardness and the presence of nanostructures and did not jeopardize titanium biocompatibility.

ACKNOWLEDGMENT

The authors would like to thank to the São Paulo Research Foundation (São Paulo, SP, Brazil) for the scholarship granted to the first author (#2010/09308-0) and for the financial support (#2010/09113-4), and to the National Council for Scientific and Technological Development (CNPq; Brasília, DF, Brazil) for the financial support (#471553/2010-7). Special thanks to Prof. Richard Landers, Gleb Wataghin Institute of Physics, State University of Campinas, Brazil, for the XPS analysis.

REFERENCES

1. Elias CN, Meirelles L. Improving osseointegration of dental implants. Expert review of medical devices. 2010;7(2):241-56.
2. Wennerberg A, Albrektsson T. On implant surfaces: a review of current knowledge and opinions. The International journal of oral & maxillofacial implants. 2010;25(1):63-74.
3. Kumazawa R, Watari F, Takashi N, Tanimura Y, Uo M, Totsuka Y. Effects of Ti ions and particles on neutrophil function and morphology. Biomaterials. 2002;23(17):3757-64.
4. Flatebo RS, Hol PJ, Leknes KN, Kosler J, Lie SA, Gjerdet NR. Mapping of titanium particles in peri-implant oral mucosa by laser ablation inductively coupled

plasma mass spectrometry and high-resolution optical darkfield microscopy. *Journal of oral pathology & medicine : official publication of the International Association of Oral Pathologists and the American Academy of Oral Pathology*. 2011;40(5):412-20.

5. Flatebo RS, Johannessen AC, Gronningsaeter AG, Boe OE, Gjerdet NR, Grung B, et al. Host response to titanium dental implant placement evaluated in a human oral model. *Journal of periodontology*. 2006;77(7):1201-10.

6. Meirelles L, Uzumaki ET, Lima JH, Muller CA, Albrektsson T, Wennerberg A, et al. A novel technique for tailored surface modification of dental implants - a step wise approach based on plasma immersion ion implantation. *Clinical oral implants research*. 2013;24(4):461-7.

7. Clem WC, Konovalov VV, Chowdhury S, Vohra YK, Catledge SA, Bellis SL. Mesenchymal stem cell adhesion and spreading on microwave plasma-nitrided titanium alloy. *Journal of biomedical materials research Part A*. 2006;76(2):279-87.

8. Bordji K, Jouzeau JY, Mainard D, Payan E, Netter P, Rie KT, et al. Cytocompatibility of Ti-6Al-4V and Ti-5Al-2.5Fe alloys according to three surface treatments, using human fibroblasts and osteoblasts. *Biomaterials*. 1996;17(9):929-40.

9. da Silva JS, Amico SC, Rodrigues AO, Barboza CA, Alves C, Jr., Croci AT. Osteoblastlike cell adhesion on titanium surfaces modified by plasma nitriding. *The International journal of oral & maxillofacial implants*. 2011;26(2):237-44.

10. Ferraz EP, Sa JC, de Oliveira PT, Alves C, Jr., Beloti MM, Rosa AL. The effect of plasma-nitrided titanium surfaces on osteoblastic cell adhesion, proliferation, and differentiation. *Journal of biomedical materials research Part A*. 2013.

11. Meirelles L, Currie F, Jacobsson M, Albrektsson T, Wennerberg A. The effect of chemical and nanotopographical modifications on the early stages of osseointegration. *The International journal of oral & maxillofacial implants*. 2008;23(4):641-7.

12. Combe EC, Owen BA, Hodges JS. A protocol for determining the surface free energy of dental materials. *Dental materials : official publication of the Academy of Dental Materials*. 2004;20(3):262-8.
13. Dodo CG, Senna PM, Custodio W, Paes Leme AF, Del Bel Cury AA. Proteome analysis of the plasma protein layer adsorbed to a rough titanium surface. *Biofouling*. 2013;29(5):549-57.
14. Goodman SB, Trindade M, Ma T, Genovese M, Smith RL. Pharmacologic modulation of periprosthetic osteolysis. *Clinical orthopaedics and related research*. 2005(430):39-45.
15. Tuan RS, Lee FY, Y TK, Wilkinson JM, Smith RL. What are the local and systemic biologic reactions and mediators to wear debris, and what host factors determine or modulate the biologic response to wear particles? *The Journal of the American Academy of Orthopaedic Surgeons*. 2008;16 Suppl 1:S42-8.
16. Bukata SV, Gelinas J, Wei X, Rosier RN, Puzas JE, Zhang X, et al. PGE2 and IL-6 production by fibroblasts in response to titanium wear debris particles is mediated through a Cox-2 dependent pathway. *Journal of orthopaedic research : official publication of the Orthopaedic Research Society*. 2004;22(1):6-12.
17. Schwarz EM, Benz EB, Lu AP, Goater JJ, Mollano AV, Rosier RN, et al. Quantitative small-animal surrogate to evaluate drug efficacy in preventing wear debris-induced osteolysis. *Journal of orthopaedic research : official publication of the Orthopaedic Research Society*. 2000;18(6):849-55.
18. Goodman SB, Davidson JA, Song Y, Martial N, Fornasier VL. Histomorphological reaction of bone to different concentrations of phagocytosable particles of high-density polyethylene and Ti-6Al-4V alloy in vivo. *Biomaterials*. 1996;17(20):1943-7.
19. De Maeztu MA, Alava JI, Gay-Escoda C. Ion implantation: surface treatment for improving the bone integration of titanium and Ti6Al4V dental implants. *Clinical oral implants research*. 2003;14(1):57-62.
20. Johansson CB, Lausmaa J, Rostlund T, Thomsen P. Commercially pure titanium and ti6al4v implants with and without nitrogen-ion implantation – surface

characterization and quantitative studies in rabbit cortical bone. Journal of materials science Materials in medicine. 1993;4:132-41.

21. Chien CC, Liu KT, Duh JG, Chang KW, Chung KH. Effect of nitride film coatings on cell compatibility. Dental materials : official publication of the Academy of Dental Materials. 2008;24(7):986-93.

22. Cortese B, Riehle MO, D'Amone S, Gigli G. Influence of variable substrate geometry on wettability and cellular responses. Journal of colloid and interface science. 2013;394:582-9.

Capítulo 3:

Evaluation of protein adsorption in vitro and bone formation in vivo on amino-functionalized titanium surface

Plinio Senna^{a,b}; Bruno Salles Sotto-Maior^c; Adriana Franco Paes Leme^d; Luiz Meirelles^b; Altair Antoninha Del Bel Cury^a

^a Department of Prosthodontics and Periodontology, Piracicaba Dental School, State University of Campinas, Avenida Limeira 901, Piracicaba, SP 13419-903, Brazil.

^b Division of Prosthodontics, Eastman Dental Center, University of Rochester, 625 Elmwood Avenue, Rochester, NY 14620, USA.

^c Department of Prosthodontics and Dental Materials, Federal University of Juiz de Fora, Juiz de Fora, Minas Gerais, Brazil. Rua José Lourenço Kelmer s/n, Juiz de Fora, MG 36036-900, Brazil.

^d Mass Spectrometry Laboratory, Brazilian Biosciences National Laboratory (LNBio), Rua Giuseppe Máximo Scolfaro 10.000, Campinas, São Paulo, 13083-970, Brazil.

Corresponding author:

Altair Antoninha Del Bel Cury

Department of Prosthodontics and Periodontology, Piracicaba Dental School, State University of Campinas. Avenida Limeira, 901. Zip Code: 13414-903. Piracicaba, São Paulo, Brazil. Phone: +55 19 21065294; Fax +55 19 2106-5211;

ABSTRACT

In the present study protein adsorption and *in vivo* bone formation were investigated on amino-functionalized titanium surface. Titanium discs (12.7×2 mm) and screw implants (3.75×6 mm) were hydroxylated by a solution of H_2SO_4 /30% H_2O_2 for 1 h and immediately amino-functionalized using 3-aminopropyltriethoxysilane (APTES). The surface topography was evaluated by scanning electron microscopy (SEM) and atomic force microscopy (AFM) and the chemical composition was identified by x-ray photoelectron spectroscopy (XPS). For protein adsorption analysis, the discs were individually incubated in 2 mL of human blood plasma for 3 h at 37°C and, after washing to remove loose proteins, the discs were pooled in a plastic tube, the adsorbed proteins were eluted and the total protein mass was quantified. In addition, 15 μg of the adsorbed proteins were analyzed by Q-TOF mass spectrometer to identify the composition of the protein layer. To evaluate bone formation, a total of 60 implants were installed in the femur/tibia of 10 New Zealand rabbits to determine bone-to-implant contact (BIC) after 3 and 6 weeks of healing. Amino-functionalization increased the nitrogen content on surface without affecting the surface topography. The total mass of adsorbed proteins was 19.9% higher on the amino-functionalized surface; however, the abundance of fibronectin was clearly reduced. BIC values showed no difference between the groups after 3 week and 6 weeks ($p > 0.05$, t test). It is possible to conclude that the amino-functionalization can alter the quantity of adsorbed proteins but this does not reflect in higher bone formation.

Keywords: Dental implants, osseointegration, aminosilane, bone formation.

INTRODUCTION

Titanium has been widely used as implant material due to its corrosion resistance and biocompatibility.¹ However, it is not bioactive and does not promote new bone formation at the early stages of healing. This may lead to early implant failure or complications during healing, especially for patient groups with the diseases such as diabetes and osteoporosis.^{2, 3} Thus, new challenges are to be faced to enhance the direct apposition of new bone at early post-implantation periods.⁴

Initial cellular interactions depend on surface physicochemical properties such as wettability, charge, heterogeneity, topography, roughness and the presence of functional groups.⁵ In this context, new focus was given to immobilize bioactive molecules to create specific cellular responses.^{6, 7} Thus, functional groups bond to the surface can work as anchoring points for attachment of other molecules and proteins.⁶ Despite there are several strategies for attaching functional amino groups to titanium, one method commonly used is the covalent bonding of 3-aminopropyltriethoxysilane (APTES) on surface.^{8, 9}

When titanium is inserted into bone, blood plasma ions and proteins adsorb first on surface and this adsorbed layer that will mediate cell adhesion.¹⁰ However, amino-functionalization by APTES can influence protein adsorption on surface and consequently all subsequent biological events up to new bone formation. Free amino groups on surface may protonate under physiological conditions, changing the surface charge at physiological condition from negative of pure titanium (pI 5.0 – 5.9) to positive of amino-functionalized titanium (pI 8.5).^{11, 12} This can increase the electrostatic interaction since most of blood plasma proteins are negatively charged (pI < 7.4).¹³ Guided by the substrate surface properties, conformational alterations of the adsorbed proteins possibly change their biological behavior.

It is difficult to assign what functional groups contributed to the adsorption process, since it involves complicated chemical reactions.¹⁴ However, the surface charge can affect the type and amount of proteins adsorbed on surface and the

ability of one protein to be displaced by others.¹⁵ Thus, changes on the protein adsorbed layer, especially on those proteins related to cell adhesion such as fibronectin and vitronectin, can influence the subsequent biological events up to new bone formation.^{16, 17.}

However, it is unknown how proteins adsorb on titanium after APTES treatment and how it influences bone formation process. Therefore, the aim in this study was to investigate protein adsorption phenomenon *in vitro* using mass spectroscopy on amino-functionalized titanium surface and to evaluate *in vivo* the influence of this treatment on new bone formation.

MATERIALS AND METHODS

Surface treatment

Titanium grade 4 was hydroxylated by H₂SO₄/30%H₂O₂ solution (1:1, v:v) for 1 h before being amino-functionalized by immersion in 10% 3-aminopropyltriethoxysilane (Sigma-Aldrich Corp., St. Louis, MO, USA) for 4 h in boiling toluene (Merck SA, Rio de Janeiro, RJ, Brazil).^{8, 18} After, the discs were washed in toluene, purified water and acetone for 10 min in each solution in an ultrasonic bath. The control group received only the acid treatment. Finally, all discs were sterilized by 25 kGy gamma radiation (CBE Embrarad, Jarinu, SP, Brazil).

Surface characterization

The surface morphology was characterized by scanning electron microscopy (SEM) (Zeiss Auriga SEM/FIB, Oberkochen, Germany) at different magnifications. Surface topography was evaluated by atomic force microscopy (Dimension Edge, Veeco Billerica, MA, EUA) using a 125 nm cantilever in tapping mode (Digital Instruments, Santa Barbara, CA, USA) and the images were digitally processed (Scanning Probe Image Processor software v.5.1.8; Image Metrology A/S, Hørsholm, Denmark). The chemical surface composition was determined by X-ray photoelectron spectroscopy (XPS) (IFGW; Unicamp, Campinas, Brazil) under 5×10^{-10} torr using monochromatic (Al K α) X-ray radiation as the exciting source.

Protein adsorption analysis

Protein adsorption was determined on discs (12.7×2 mm), which were individually placed into a 24-well sterile plate to be incubated with 2 mL of human blood plasma for 180 min at 37°C in an orbital shaker according to a previous study.¹³ Briefly, the discs were washed after the incubation time to remove unbound proteins and pooled ($n = 12$) into a polypropylene tube containing 20 mL of purified water. Each tube was vortexed for 1 min and sonicated for 5 min (7 W/4 °C) to elute the adsorbed proteins from the surface. The suspension was collected and lyophilized. The total protein mass was quantified using the Bradford method (Bio-Rad, Hercules, CA, USA) using bovine serum albumin standards (Sigma-Aldrich Corp.).¹⁹ Data was analyzed by *t* test at a significance level of 5% ($n = 5$).

Next, a volume equivalent to 15 µg of the extracted proteins was lyophilized again to be identified and quantification by mass spectroscopy (LC-MS/MS). For this, the proteins were reduced, alkylated and digested with trypsin (1:50, w/w).²⁰ The resulting peptides were resuspended in 12 µL of 0.1% formic acid and then separated at a flow rate of 0.6 µL/min by C18 (100 µm x 100 mm) RPNanoUPLC (nanoAcquity; Waters Corp., Milford, MA, USA) coupled to a mass spectrometer (Q-ToF Ultima; Waters Corp.) with a nanoelectrospray (ESI) source.

The identified amino acids sequences (Mascot Distiller 2009; Matrix Science Inc., Boston, MA, USA). were matched against the Human International Protein Database (IPI) (v.3.72).²¹ Only peptides with a minimum of five amino acid residues which showed significant threshold ($p < 0.05$) in Mascot-based score were considered in the results.

Bone formation analysis

Threaded implants (3.75×6 mm) with external hexagon platform (P-I Brånemark Philosophy, São Paulo, SP, Brazil) were inserted in a total of 10 New Zealand White rabbits (9 months of age). This study was approved by the local Ethical Committee of University of Rochester, NY, USA. Each rabbit received one implant in each distal femoral metaphysis and two in each proximal tibial metaphysis

(3 experimental and 3 control implants randomly distributed). The animals were kept in separate cages during the whole experiment with free access to tap water and standard diet.

The implants were placed under general anaesthesia (0.3 mg/ml intramuscular fentanyl and 10 mg/ml fluanisone followed by 2.5 mg intraperitoneal diazepam). The legs were shaved and disinfected with chlorhexidin before injection of 1 ml of lidocain into each insertion site. The skin and fascial layers were opened and bone drilling was performed at low speed and profuse saline cooling. After implant insertion, the fascial layers were closed with absorbable suture while skin layer with polypropylene. All animals were allowed to bear their full body weight immediately after surgery.

The animals were sacrificed after 3 and 6 weeks of healing with Pentobarbital Vet (Apoteket AB, Stockholm, Sweden) after sedation. A total of 40 implants were placed in the tibia (10 implants/group/timepoint), while in the femur a total of 20 implants were placed (5 implants/group/timepoint). The implants and surrounding bone were removed and fixed with 4% neutral buffered formaldehyde. The specimens were embedded in light curing resin (Technovit 7200 VLC, KÜltzer & Co, Germany) after dehydration in graded series of ethanol. A section of the midline of each implant was obtained and ground up to 20 µm thick (two cell layers).

After toluidine blue staining, the bone-to-implant contact (BIC) area was measured by a blind examiner using a microscope (80i; Nikon Instruments, USA) equipped with an image software analysis (NIS-Elements BR 3.2, Nikon, USA). BIC data was analyzed by *t* test at a significance level of 5%.

RESULTS

The morphological surface characteristics are showed in Figures 1 and 2. SEM images showed a similar minimally rough surface, due to the hydroxylation treatment with sulfuric acid and hydrogen peroxide, on both titanium surfaces. Also, the tridimensional reconstructions of AFM data revealed similar pattern of nanostructures on both surfaces.

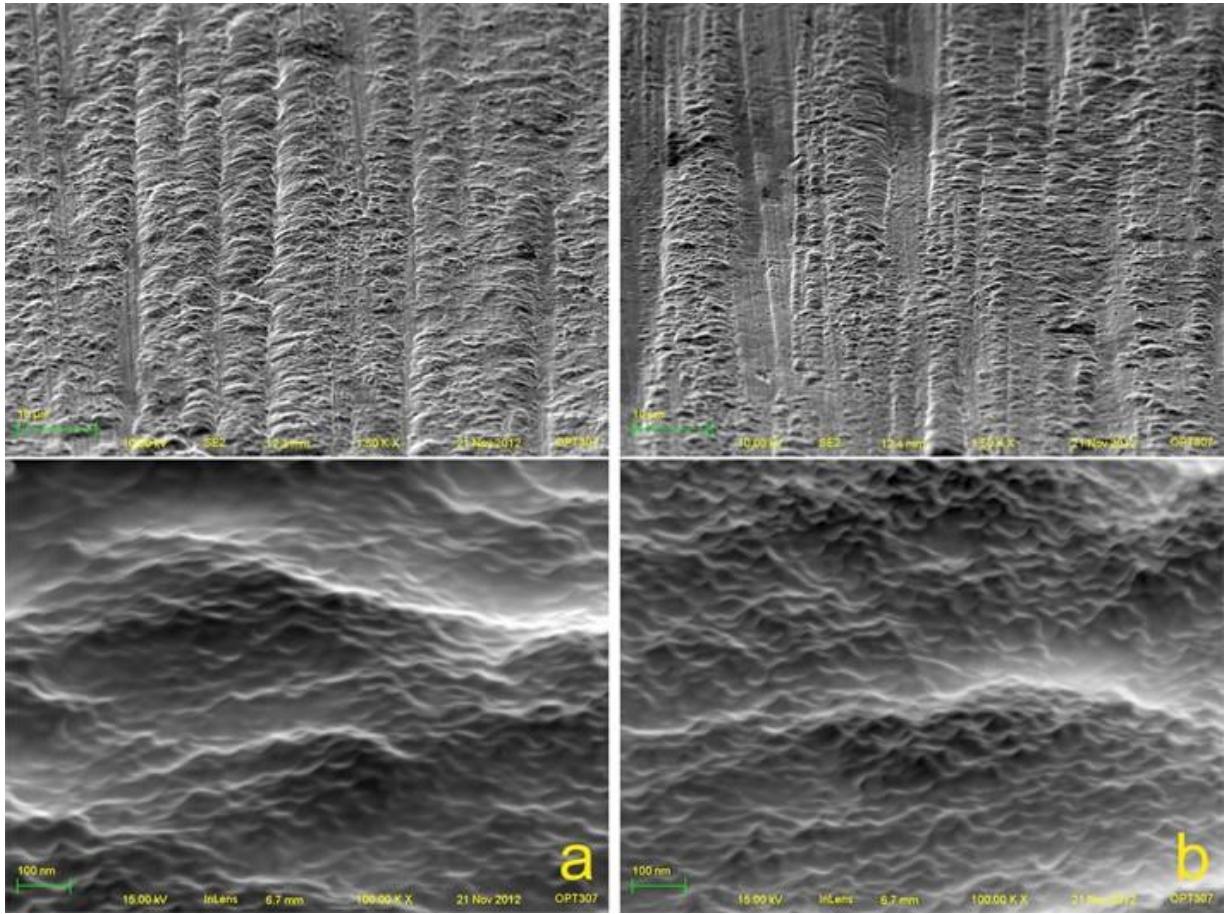


Figure 1. SEM images of titanium (a) and amino-functionalized titanium (b), showing similar surface morphology.

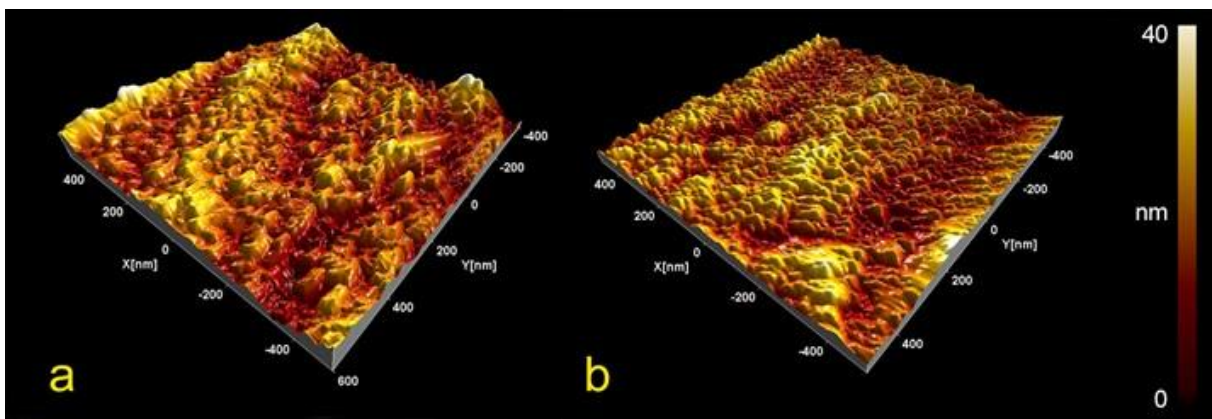


Figure 2. Tridimensional reconstruction of AFM data of titanium (a) and amino-functionalized titanium (b), showing similar average roughness deviation (S_a) 75.0 ± 32.7 and 88.0 ± 31.1 nm, respectively ($p > 0.05$, t test).

The XPS diffractograms are presented in Figure 3. Small signals of nitrogen and silicon were detected on titanium after amino-functionalization treatment, which indicated the presence of a submonolayer to monolayer of APTES bond on the surface.

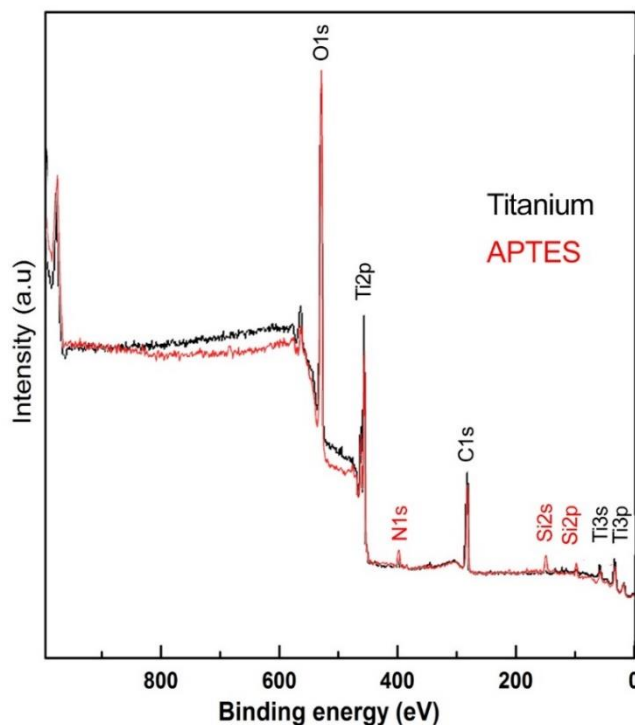


Figure 3. XPS diffractograms of titanium and amino-functionalized titanium.

The total protein mass present on conditioning film onto the amino-functionalized titanium were almost 19.9% higher than the titanium surface (23.56 ± 0.49 and $19.64 \pm 0.58 \mu\text{g}/\text{cm}^2$, respectively) ($p < 0.05$). However, lower relative abundance of fibronectin was identified after APTES treatment (Tables 1 and 2).

Table 1. Proteins identified by LC-MS/MS on the titanium surface.

#	Accession number	Protein	MW (Da)	Mascot Score	Unique peptides	Spectral counts	emPAI
1	IPI00022418	Fibronectin (isoform 1)	266052	4263	26	83	0.41
	IPI00922213	Fibronectin (transcript variant)	112204	3022	15	57	0.63
	IPI00983517	Fibronectin (FN1)	26596	391	3	6	0.42
2	IPI00022434	Serum Albumin	73881	1139	18	35	1.19
3	IPI00021841	Apolipoprotein A-I	30759	1040	10	21	1.05
4	IPI00298497	Fibrinogen (β chain)	56577	927	8	18	0.76
	IPI00021885	Fibrinogen (α chain)	95656	795	4	12	0.14
	IPI00021891	Fibrinogen (γ chain)	52106	717	6	14	0.63
5	IPI00384938	Putative uncharacterized protein DKFZp686N02209	53503	635	5	9	0.35
6	IPI00383164	SNC66 protein	54601	442	3	7	0.19
7	IPI00478493	HP protein	38940	230	5	11	0.39
8	IPI00003269	β -actin-like protein	42318	184	1	3	0.08
9	IPI00478003	α_2 -Macroglobulin	164613	165	2	4	0.04
10	IPI00032220	Angiotensinogen	53406	124	2	4	0.06
11	IPI00783987	Complement C3	188569	121	2	4	0.02
12	IPI00022488	Hemopexin	52385	102	1	3	0.06
13	IPI00399007	Putative uncharacterized protein DKFZp686I04196	46716	87	2	3	0.07
14	IPI00032258	Complement C4-A	194247	82	2	3	0.02
15	IPI00017601	Ceruloplasmin	122983	63	2	2	0.05
16	IPI00298971	Vitronectin	55069	53	1	2	0.06
17	IPI00021854	Apolipoprotein A-II	11282	46	3	4	0.70
18	IPI00385264	Immunoglobulin (μ heavy chain - C region)	43543	29	1	1	0.08
19	IPI00026944	Nidogen-1	139142	28	1	1	0.02
20	IPI00004838	Adapter molecule crk	33867	26	1	1	0.10
21	IPI00218658	Inositol 1,4,5-trisphosphate receptor	315345	24	1	5	0.01
22	IPI00218784	Sphingomyelin phosphodiesterase	70790	23	1	10	0.05
23	IPI00022417	Leucine-rich α_2 -glycoprotein	38382	22	1	3	0.09
24	IPI00187091	MAP interacting serine/threonine-protein kinase	48056	17	1	3	0.07
25	IPI00553177	α_1 -Antitrypsin	46878	15	1	1	0.07

MW – Molecular weight (Da); Mascot score – probability score; Unique peptides– number of unique peptides identified per protein; Spectral counts - number of MS/MS spectra obtained for a protein; emPAI – Exponentially modified protein abundance index.

Table 2. Proteins identified by LC-MS/MS on the amino-functionalized titanium surface.

#	Accession number	Protein	MW (Da)	Mascot Score	Unique peptides	Spectral counts	emPAI
1	IPI00021841	Apolipoprotein A-I	30759	2476	10	51	3.06
2	IPI00384938	Putative uncharacterized protein DKFZp686N02209	53503	1692	4	27	0.78
3	IPI00022434	Serum albumin	73881	1593	13	57	1.92
4	IPI00383164	SNC66 protein	54601	775	4	11	0.38
5	IPI00298497	Fibrinogen (β chain)	56577	615	6	18	0.67
	IPI00021885	Fibrinogen (α chain)	95656	211	8	9	0.17
	IPI00021891	Fibrinogen (γ chain)	52106	203	3	4	0.19
6	IPI00032258	Complement C4-A	194247	472	4	10	0.10
7	IPI00930442	Putative uncharacterized protein DKFZp686M24218	53071	415	2	6	0.13
8	IPI00641737	Haptoglobin	45861	316	9	14	0.63
9	IPI00022488	Hemopexin	52385	277	2	7	0.26
10	IPI00478493	HP protein	38940	164	5	9	0.5
11	IPI00032220	Angiotensinogen	53406	139	2	3	0.12
12	IPI00017601	Ceruloplasmin	122983	133	1	6	0.08
13	IPI00003269	β -actin-like protein	42318	90	2	2	0.08
14	IPI00399007	Putative uncharacterized protein DKFZp686I04196	46716	89	1	1	0.07
15	IPI00783987	Complement C3	188569	80	4	7	0.05
16	IPI00479743	POTE ankyrin domain family member E	122882	75	2	2	0.03
17	IPI00021854	Apolipoprotein A-II	11282	61	2	3	0.70
18	IPI00022431	α_2 -HS-glycoprotein (chain A)	47567	55	1	1	0.07
19	IPI00032328	Kininogen-1	72996	51	1	2	0.08
20	IPI00022418	Fibronectin (isoform 1)	266052	45	1	2	0.01
21	IPI00022463	Serotransferrin	79294	41	1	1	0.04
22	IPI00006114	Pigment epithelium-derived factor	46454	40	1	1	0.07
23	IPI00022417	Leucine-rich α_2 -glycoprotein	38382	28	1	2	0.09
24	IPI00026944	Nidogen-1	139142	28	1	1	0.02
25	IPI00000151	Integrin $\beta 6$	89244	26	1	1	0.04
26	IPI00303746	Probable ATP-dependent RNA helicase DHX58	77477	15	1	2	0.04

MW – Molecular weight (Da); Mascot score – probability score; Unique peptides– number of unique peptides identified per protein; Spectral counts - number of MS/MS spectra obtained for a protein; emPAI – Exponentially modified protein abundance index.

Considering the bone response, no inflammatory response or adverse reaction was seen around the implants. The implant site in the femur consisted mainly of trabecular bone whereas tibial sites were characterized by a cortical layer of 1.5 mm in height. After 3 weeks, both implants showed typical endosteum reaction leading to new bone down growth from the cortical layer and after 6 weeks of healing, the newly formed mineralized tissue contains osteocytes and osteoblast seams indicating continuous mineralization of the tissue. Histomorphometric analyses showed similar BIC values for both implants ($p > 0.05$) after 3 and 6 weeks (Figure 4).

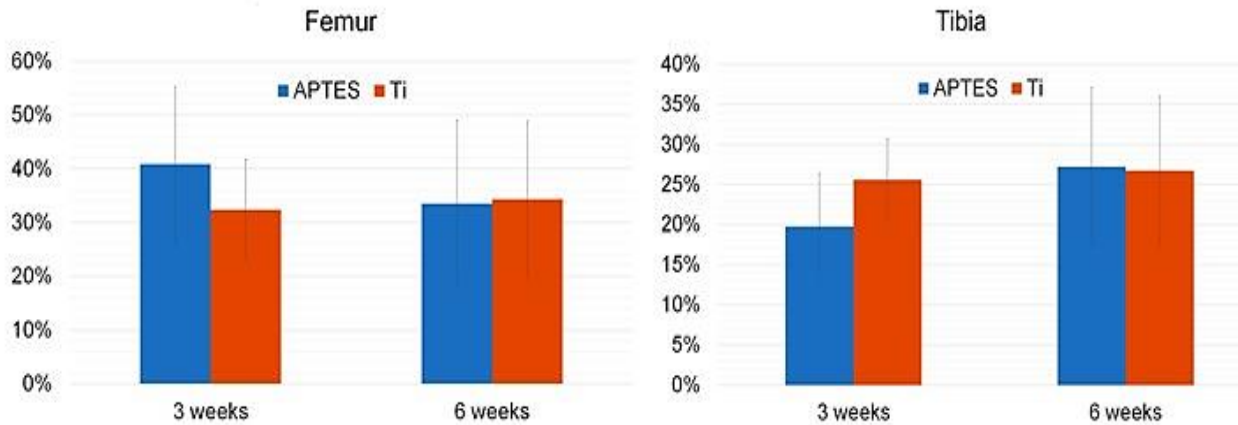


Figure 4. BIC values of amino-functionalized implants placed on the femur and tibia of rabbits after 3 and 6 weeks of healing.

DISCUSSION

The findings from the present study indicated that the increase of unspecific protein adsorption on surface promoted by APTES does not reflect in early bone formation. Despite amino-functionalization allowed a higher quantity of total proteins adsorbed on surface, the implants failed to show signs of early mineralization and the threads were mainly filled by coagulum at 3 weeks healing.

After 6 weeks, similar bone formation was observed starting from the endosteum due to the disruption of blood vessels.^{22, 23}

The surgical protocol and implant design were identical for both implant groups. The surface topography was also similar due to the acid treatment for hydroxylation needed for further silanization. Thus, the only variable was the presence of the APTES layer on the surface. The hypothesis that amino-functionalization treatment could enhance early bone formation was rejected, corroborating a previous study that showed lower cell adhesion after silanization.²⁵

Previous studies evaluating APTES coating reported a coverage from 0.25 to 5 nmol/cm² on TiO₂.^{6, 12, 24} However, it did not reflected in higher bone formation. This can be explained by the low hydrolytic stability of the siloxane bond to titanium, which makes the aminosilane monolayer is more accessible for hydrolytic attack when in contact with blood. Previous study showed that silane monolayer of samples left in water degraded within 11 days; however, it was not evaluated at physiological pH.²⁵ Thus, the immediate effect of APTES on protein adsorption was not enough to stimulate early bone formation over time.

The current findings revealed that the monolayer of APTES on surface was able to increase the quantity of adsorbed proteins on titanium. This confirms that adsorption occurs more easily on surfaces with higher energy and reactivity.¹⁴ Although blood has more than 150 proteins, the most abundant proteins and with the highest diffusion coefficient, that would be first to arrive and adsorb on the surface,²⁶ were not necessarily present on surface with the same blood concentration. Thus, albumin, IgG, α_1 -Antitrypsin and fibrinogen were not the most abundant proteins within the adsorbed layer. The post adsorption phenomenon referred as the Vroman effect, which shows that some molecules can be removed by others, may explain this occurrence.²⁷

Although few studies assessed the competitive behavior of protein adsorption on titanium from human blood plasma,²⁸⁻³⁰ the present study showed some changes on concentration of adsorbed proteins when APTES was used. The higher content of albumin on APTES group confirms previous data that its

adsorption depends on the presence of polar groups of surface.¹⁰ However, fibronectin abundance in the adsorbed proteins layer was clearly reduced on APTES group.

Fibronectin is a glycoprotein that promotes attachment of cells to the biomaterial surface through its central-binding domain RGD sequence, that is recognized by integrin receptors present in cell membrane.³¹ The lack of this protein on surface may also contributed to the similar bone formation found in the present study. Thus, cell adhesion on APTES group was mainly dependent of the fibrin scaffold developed after fibrinogen adsorption.

The vagaries of competitive protein adsorption may not be left to the host tissue, since biological activity of adsorbed proteins can be modulated by the substrate though differences in protein conformation that affects the availability of binding domains.³² Despite conformational changes are reported, this type of analysis was beyond the scope of the current study. Thus, unspecific adsorption should be avoided and the surface should be designed to have specific interaction pathway for a promising route toward controlled bone formation on titanium.

CONCLUSION

Amino-functionalization of titanium surface increased the adsorption of plasma proteins but it did not reflect in higher bone formation.

ACKNOWLEDGMENT

The authors would like to thank to the São Paulo Research Foundation (São Paulo, SP, Brazil) for the scholarship granted to the first author (#2010/09308-0) and for the financial support (#2010/09113-4), and to the National Council for Scientific and Technological Development (CNPq; Brasília, DF, Brazil) for the financial support (#471553/2010-7). Special thanks to Prof. Richard Landers, Gleb Wataghin Institute of Physics, State University of Campinas, Brazil, for the XPS analysis.

REFERENCES

1. Cai K, Frant M, Bossert J, Hildebrand G, Liefelth K, Jandt KD. Surface functionalized titanium thin films: zeta-potential, protein adsorption and cell proliferation. *Colloids and surfaces*. 2006;50(1):1-8.
2. van Steenberghe D, Jacobs R, Desnyder M, Maffei G, Quirynen M. The relative impact of local and endogenous patient-related factors on implant failure up to the abutment stage. *Clinical oral implants research*. 2002;13(6):617-22.
3. Johnsen SP, Sorensen HT, Lucht U, Soballe K, Overgaard S, Pedersen AB. Patient-related predictors of implant failure after primary total hip replacement in the initial, short- and long-terms. A nationwide Danish follow-up study including 36,984 patients. *J Bone Joint Surg Br*. 2006;88(10):1303-8.
4. Park JW, Kurashima K, Tustusmi Y, An CH, Suh JY, Doi H, et al. Bone healing of commercial oral implants with RGD immobilization through electrodeposited poly(ethylene glycol) in rabbit cancellous bone. *Acta biomaterialia*. 2011;7(8):3222-9.
5. Rabe M, Verdes D, Seeger S. Understanding protein adsorption phenomena at solid surfaces. *Advances in colloid and interface science*. 2011;162(1-2):87-106.
6. Dettin M, Bagno A, Gambaretto R, Iucci G, Conconi MT, Tuccitto N, et al. Covalent surface modification of titanium oxide with different adhesive peptides: surface characterization and osteoblast-like cell adhesion. *Journal of biomedical materials research Part A*. 2009;90(1):35-45.
7. Adden N, Gamble LJ, Castner DG, Hoffmann A, Gross G, Menzel H. Phosphonic acid monolayers for binding of bioactive molecules to titanium surfaces. *Langmuir : the ACS journal of surfaces and colloids*. 2006;22(19):8197-204.
8. Nanci A, Wuest JD, Peru L, Brunet P, Sharma V, Zalzal S, et al. Chemical modification of titanium surfaces for covalent attachment of biological molecules. *Journal of biomedical materials research*. 1998;40(2):324-35.
9. Matinlinna JP, Areva S, Lassila LVJ, Vallittu PK. Characterization of siloxane films on titanium substrate derived from three aminosilanes. *Surface and Interface Analysis*. 2004;36(9):1314-22.

10. Feng B, Weng J, Yang BC, Qu SX, Zhang XD. Characterization of titanium surfaces with calcium and phosphate and osteoblast adhesion. *Biomaterials*. 2004;25(17):3421-8.
11. Imamura K, Shimomura M, Nagai S, Akamatsu M, Nakanishi K. Adsorption characteristics of various proteins to a titanium surface. *J Biosci Bioeng*. 2008;106(3):273-8.
12. Sakey M, Smatt JH. Comparison of different amino-functionalization procedures on a selection of metal oxide microparticles: degree of modification and hydrolytic stability. *Langmuir : the ACS journal of surfaces and colloids*. 2012;28(49):16941-50.
13. Dodo CG, Senna PM, Custodio W, Paes Leme AF, Del Bel Cury AA. Proteome analysis of the plasma protein layer adsorbed to a rough titanium surface. *Biofouling*. 2013;29(5):549-57.
14. Feng B, Weng J, Yang BC, Qu SX, Zhang XD. Characterization of surface oxide films on titanium and adhesion of osteoblast. *Biomaterials*. 2003;24(25):4663-70.
15. Kabaso D, Gongadze E, Perutkova S, Matschegewski C, Kralj-Iglic V, Beck U, et al. Mechanics and electrostatics of the interactions between osteoblasts and titanium surface. *Computer methods in biomechanics and biomedical engineering*. 2011;14(5):469-82.
16. Macdonald W, Campbell P, Fisher J, Wennerberg A. Variation in surface texture measurements. *Journal of biomedical materials research Part B, Applied biomaterials*. 2004;70(2):262-9.
17. Nebe B, Finke B, Luthen F, Bergemann C, Schroder K, Rychly J, et al. Improved initial osteoblast functions on amino-functionalized titanium surfaces. *Biomolecular engineering*. 2007;24(5):447-54.
18. Bagno A, Piovan A, Dettin M, Brun P, Gambaretto R, Palu G, et al. Improvement of Anselme's adhesion model for evaluating human osteoblast response to peptide-grafted titanium surfaces. *Bone*. 2007;41(4):704-12.

19. Bradford MM. A rapid and sensitive method for the quantitation of microgram quantities of protein utilizing the principle of protein-dye binding. *Anal Biochem.* 1976;72(1-2):248-54.
20. Paes Leme AF, Escalante T, Pereira JG, Oliveira AK, Sanchez EF, Gutierrez JM, et al. High resolution analysis of snake venom metalloproteinase (SVMP) peptide bond cleavage specificity using proteome based peptide libraries and mass spectrometry. *Journal of proteomics.* 2011;74(4):401-10.
21. Kersey PJ, Duarte J, Williams A, Karavidopoulou Y, Birney E, Apweiler R. The International Protein Index: an integrated database for proteomics experiments. *Proteomics.* 2004;4(7):1985-8.
22. McKibbin B. The biology of fracture healing in long bones. *J Bone Joint Surg Br.* 1978;60-B(2):150-62.
23. Roberts WE. Bone tissue interface. *J Dent Educ.* 1988;52(12):804-9.
24. Rosenholm JM, Lindén M. Wet-Chemical Analysis of Surface Concentration of Accessible Groups on Different Amino-Functionalized Mesoporous SBA-15 Silicas. *Chemistry of Materials.* 2007;19(20):5023-34.
25. Pegg EC, Walker GS, Scotchford CA, Farrar D, Grant D. Mono-functional aminosilanes as primers for peptide functionalization. *Journal of biomedical materials research Part A.* 2009;90(4):947-58.
26. Yoshinari M, Oda Y, Kato T, Okuda K, Hirayama A. Influence of surface modifications to titanium on oral bacterial adhesion in vitro. *Journal of biomedical materials research.* 2000;52(2):388-94.
27. Noh H, Vogler EA. Volumetric interpretation of protein adsorption: competition from mixtures and the Vroman effect. *Biomaterials.* 2007;28(3):405-22.
28. Oughlis S, Lessim S, Changotade S, Bollotte F, Poirier F, Helary G, et al. Development of proteomic tools to study protein adsorption on a biomaterial, titanium grafted with poly(sodium styrene sulfonate). *Journal of chromatography B, Analytical technologies in the biomedical and life sciences.* 2011.
29. Gillich T, Benetti EM, Rakhmatullina E, Konradi R, Li W, Zhang A, et al. Self-assembly of focal point oligo-catechol ethylene glycol dendrons on titanium oxide

surfaces: adsorption kinetics, surface characterization, and nonfouling properties. Journal of the American Chemical Society. 2011;133(28):10940-50.

30. Sela MN, Badihi L, Rosen G, Steinberg D, Kohavi D. Adsorption of human plasma proteins to modified titanium surfaces. Clinical oral implants research. 2007;18(5):630-8.

31. Bergkvist M, Carlsson J, Oscarsson S. Surface-dependent conformations of human plasma fibronectin adsorbed to silica, mica, and hydrophobic surfaces, studied with use of Atomic Force Microscopy. Journal of biomedical materials research Part A. 2003;64(2):349-56.

32. Sousa SR, Moradas-Ferreira P, Barbosa MA. TiO₂ type influences fibronectin adsorption. Journal of materials science Materials in medicine. 2005;16(12):1173-8.

Considerações gerais

Há um esforço por parte da ciência em se determinar os parâmetros ideais de superfície dos implantes, assim como propor novos meios de tornar a superfície do titânio bioativa. Como a utilização das superfícies moderadamente rugosas pode gerar partículas soltas na interface osso-implante, novos tratamentos de superfície devem ser investigados.

Neste trabalho, demonstrou-se a presença de partículas de titânio e alumínio na interface osso-implante após o procedimento de inserção no tecido ósseo. No entanto, a resposta biológica frente a esta ocorrência deve ser investigada em futuros estudos. Como forma de minimizar a geração de partículas, também foi avaliado neste estudo a biocompatibilidade da titânio após tratamento de nitretação por plasma. Apesar, de mostrar-se biocompatível, novos estudos são necessários para validar este tratamento como forma de evitar a geração de partículas durante a instalação dos implantes.

No presente estudo, ainda foi avaliado os efeitos da amino-funcionalização da superfície na adsorção de proteínas e na osteogênese, no qual a mudança do potencial elétrico na superfície poderia ser uma alternativa para estimular a osseointegração sem depender da topografia da superfície. No entanto, acaba estimulando a adsorção de proteínas na superfície de maneira inespecífica, o que acaba por não trazer benefício direto para a formação óssea inicial ao redor dos implantes.

Assim, novos estudos são necessários para o desenvolvimento de superfícies bioativas que estimulem a osseointegração.

Conclusão

Dentro das limitações deste estudo, pode-se concluir que: (1) superfícies moderadamente rugosas comerciais podem gerar partículas soltas de titânio e alumínio na interface osso-implante; (2) a nitretação por plasma a frio não prejudica a biocompatibilidade do titânio; e (3) a amino-funcionalização aumenta a adsorção de proteínas sobre o titânio mas não é capaz de estimular a formação óssea inicial.

Referências *

1. Albrektsson T, Sennerby L. Direct bone anchorage of oral implants: clinical and experimental considerations of the concept of osseointegration. *Int J Prosthodont*. 1990;3(1):30-41.
2. Zinger O, Zhao G, Schwartz Z, Simpson J, Wieland M, Landolt D, et al. Differential regulation of osteoblasts by substrate microstructural features. *Biomaterials*. 2005;26(14):1837-47.
3. Kubo K, Tsukimura N, Iwasa F, Ueno T, Saruwatari L, Aita H, et al. Cellular behavior on TiO₂ nanonodular structures in a micro-to-nanoscale hierarchy model. *Biomaterials*. 2009;30(29):5319-29.
4. Wennerberg A, Albrektsson T. On implant surfaces: a review of current knowledge and opinions. *Int J Oral Maxillofac Implants*. 2010;25(1): 63-74.
5. Kumazawa R, Watari F, Takashi N, Tanimura Y, Uo M, Totsuka Y. Effects of Ti ions and particles on neutrophil function and morphology. *Biomaterials*. 2002;23(17):3757-64.
6. Flatebo RS, Hol PJ, Leknes KN, Kosler J, Lie SA, Gjerdet NR. Mapping of titanium particles in peri-implant oral mucosa by laser ablation inductively coupled plasma mass spectrometry and high-resolution optical darkfield microscopy. *J Oral Pathol Med*. 2011;40(5):412-20.
7. Flatebo RS, Johannessen AC, Gronningsaeter AG, Boe OE, Gjerdet NR, Grung B, et al. Host response to titanium dental implant placement evaluated in a human oral model. *J of Periodontol*. 2006;77(7):1201-10.
8. Rastkar AR, Kiani A, Alvand F, Shokri B, Amirzadeh M. Effect of pulsed plasma nitriding on mechanical and tribological performance of Ck45 steel. *J Nanosci Nanotechnol*. 2011;11(6):5365-73.

* De acordo com as normas da UNICAMP/FOP, baseadas na padronização do International Committee of Medical Journal Editors. Abreviatura dos periódicos em conformidade com o Medline.

9. Baier RE, Meyer AE. Future directions in surface preparation of dental implants. *J Dent Educ.* 1988;52(12):788-91.
10. Nanci A, Wuest JD, Peru L, Brunet P, Sharma V, Zalzal S, et al. Chemical modification of titanium surfaces for covalent attachment of biological molecules. *J Biomed Mater Res.* 1998;40(2):324-35.
11. Nebe B, Finke B, Luthen F, Bergemann C, Schroder K, Rychly J, et al. Improved initial osteoblast functions on amino-functionalized titanium surfaces. *Biomol Eng.* 2007;24(5):447-54.
12. Okada, M., et al., Optimization of amino group density on surfaces of titanium dioxide nanoparticles covalently bonded to a silicone substrate for antibacterial and cell adhesion activities. *J Biomed Mater Res A.* 2006. 76(1): p. 95-101.

Anexo 1: Certificado de aprovação do Comitê de Ética em Pesquisa Animal



EASTMAN DENTAL CENTER
SCHOOL OF MEDICINE AND DENTISTRY
SCHOOL OF NURSING
STRONG MEMORIAL HOSPITAL
UNIVERSITY MEDICAL FACULTY GROUP

THE UNIVERSITY COMMITTEE ON ANIMAL RESOURCES

Verification of Protocol Review and Approval

University of Rochester
University Committee on Animal Resources

Title of Application: **Effect of loose titanium particles on initial bone formation around titanium implants**

Principal Investigators: **Luiz Meirelles, Ph.D.**

Name of Institution: **University of Rochester**

PHS Assurance: **A-3292-01**

Species: **Rabbit**

Protocol Number: **101443 / 2012-006**

Status: **Approved**

Approval Date: **March 15, 2012**

This letter certifies that the above protocol has been reviewed and approved by the University Committee on Animal Resources (UCAR). The protocol is effective for three (3) years from the date of approval. The approval date will be used as the anniversary date for Annual Protocol Reviews. The protocol may be subject to suspension if the conditions and requirements of the UCAR are not met.

Signed:

A handwritten signature in cursive script, reading "Suzanne Y. Stevens".

March 15, 2012

Suzanne Y. Stevens, Ph.D., UCAR Chair
or Christopher Stodgell, Ph.D., UCAR Vice-Chair
or Diane Moorman-White, D.V.M.
or Jeffrey D. Wyatt, D.V.M., M.P.H.

601 Elmwood Avenue, Box 674
Rochester, New York 14642
(Office) 585-275-1693 (Fax) 585-273-1337
E-mail: ucar@urmc.rochester.edu